Stony Brook University

Synthesis and Characterization of Iodine laden Graphene Nano Platelets *via* reduction of Graphene Oxide Using Hydrogen Iodide

A Thesis Presented

by

Joe Livingston Sundararaj

to

The Graduate School

in Partial Fulfillment of the

Requirements

for the Degree of

Master of Science

in

Materials Science and Engineering

Stony Brook University

May 2012

Stony Brook University

The Graduate School

Joe Livingston Sundararaj

We, the thesis committee for the above candidate for the

Master of Science degree, hereby recommend

acceptance of this thesis.

Dr. Balaji Sitharaman – Thesis Advisor
Assistant Professor, Biomedical Engineering

Dr. Dilip Gersappe
Associate Professor, Materials Science and Engineering

Dr. Terry Button
Associate Professor of Radiology, Stony Brook Medical Center

This thesis is accepted by the Graduate School

Charles Taber
Interim Dean of the Graduate School

Abstract of the Thesis

SYNTHESIS AND CHARACTERIZATION OF IODINE LADEN GRAPHENE NANO PLATELETS THROUGH REDUCTION OF GRAPHENE OXIDE USING HYDROGEN IODIDE

by

Joe Livingston Sundararaj

Master of Science
in
Materials Science and Engineering

Stony Brook University
2012

This research thesis proposes a novel method for the synthesis, analysis and characterization of Iodinated X-Ray contrast agents using Graphene Nanoplatelets (GNPs) for Computed Tomographic Imaging. Graphene Oxide was synthesized using the Hummers Method of Oxidation [1] through oxidative treatment of Graphite with Potassium Permanganate ($KMnO_4$). The resulting Graphene Oxide was chemically reduced using varying concentrations of Hydrogen Iodide *or* Hydroiodic acid (HI), rather than the conventionally used highly toxic Hydrazine Hydrate (N_2H_4) to strip off the oxygen functionalities. In the process of chemical reduction using Hydrogen Iodide, we hypothesized that this would result in the incorporation of Iodine into the Graphitic structure. Raman Spectroscopy, EDS along with XRD analysis provided evidence for the reduction of GO. Raman spectra for reduced GNPs showed an increase in I_D/I_G ratio from that of graphene oxide and also a peak at 154cm^{-1} attributed to I_5^-. EDS/EDX spectra for HI reduced GO showed a peak at X-ray energy level 3.94KeV characteristic of Iodine. Further analysis using Ion-Selective Electrode measurements confirmed the presence of about 10% Iodine in the Hydroiodic acid reduced samples. SEM and TEM images showed a brief morphology of the Graphene Nanoplatelets. Finally, to elucidate the possibility of Iodinated GNPs to be developed into potential CT contrast agents in the near or far future, CT Phantoms of Iodine loaded GNPs at a concentration of 40mg/ml in water showed excellent contrast density with water and dilute Hydroiodic acid as controls.

~For *Appa* and *Amma*~

Table of Contents

Figure	List of Figures	Page
1.1	2-dimensional illustrative view of single layer Graphene showing hexagonal arrangement of carbon atoms. Source: Lawrence Berkeley National Laboratory	4
1.2	Structural model of Graphene Oxide. Reprinted from literature	6
2.1	Photograph of (a) Graphite and GO in water (b) Graphite and GO in water after 10 minutes; high water solubility of Graphene oxide	19
2.2	The structure of Hydrazine Hydrate. Source: Andrew R. Barron, *The Connexions Project*	20
2.3	SEM Image of Graphene Oxide synthesized through the modified Hummer's method	23
2.4	SEM Images of (a) N_2H_4 reduced GO (b) 8.025mM HI reduced GO (c) 16.05mM HI reduced GO (d) 32.1mM HI reduced GO	24
2.5	(a) 32.1mM HI reduced GNP –powder sample (b) 32.1mM HI reduced spin coated sample showing stacked layers	25
2.6	Low resolution TEM images of HI reduced Graphene Nano Platelets at low magnification	26
2.7	Low resolution TEM images of HI reduced Graphene Nano Platelets at high magnification showing single or few layers of graphene nano sheets	28
2.8	High Resolution TEM images of HI reduced Graphene Nano Platelets (a) 5nm level magnification (b) 10nm level magnification (c) and (d) 2nm level magnification	29
2.9	Inner shell electron ionization in an atom and subsequent de-excitation by electron transitions	31
2.10a	EDS Spectrum of Graphene Oxide bulk powder showing Oxygen peak at 0.52KeV along with peaks for Manganese and Potassium EDS	32
2.10b	Spectrum of Hydrazine Reduced Graphene nano platelets bulk powder showing reduction in Oxygen peak and residual Manganese peak	32

Scheme	List of Schemes	Page
1.1	Proposed epoxide reduction reaction mechanism using Hydrazine Hydrate (N_2H_4). Reprinted from literature	7

Table	List of Tables	Page

List of Abbreviations/ Chemical names

ACS	American Chemical Society
AFM	Atomic Force Microscopy
ASTM	American Society for Testing and Materials
CA	Contrast Agent
CH_30H	Methanol
CH_3COCH_3	Acetone
CNT	Carbon Nano Tubes
CT	Computed Tomography
Dextran T_6 or T_{10}	Dextran Technical Grade 6 or Technical Grade 10
DI water	Deionized water
EDS/EDX	Energy Dispersive X-Ray Spectroscopy
EELS	Electron Energy Loss Spectroscopy
FTIR	Fourier Transform Infrared Spectroscopy
GNP	Graphene Nano Platelets
GNR	Graphene Nano Ribbons
GONP	Graphene Oxide Nano Platelets
H_2SO_4	Sulphuric Acid
HCOOH	Formic Acid
HI	Hydrogen Iodide or Hydroiodic Acid
HNO_3	Nitric Acid
HR-TEM	High Resolution - Transmission Electron Microscopy

HU	Hounsfield Units
I_2GNPs	Iodine laden Graphene Nano Platelets
I_3^-	Triiodide
I_5^-	Pentaiodide
ICDD	The International Centre for Diffraction Data
ICP	Inductively Coupled Plasma
ICP-OES	Inductively Coupled Plasma – Optical Emission Spectrometry
ISO	International Organization for Standardization
KeV	Kilo electron volt
KMnO4	Potassium Permanganate
MRI	Magnetic Resonance Imaging
N_2H_4	Hydrazine Hydrate
NaBH4	Sodium Borohydrate
Nd:YAG	Neodymium-doped Yttrium Aluminium Garnet
O/C	Oxygen to Carbon ratio
OC	Oxidative Combustion
RPM	Revolutions per minute
SEM	Scanning Electron Microscope
STEM	Scanning transmission electron microscope
TEM	Transmission Electron Microscope
TGA	Thermo Gravimetric Analysis
VCT	Volume Computed Tomography

Acknowledgments

A famous American theoretical physicist, often called ‘Father of the Atomic Bomb’ once said, “In the material sciences these are and have been, and are most surely likely to continue to be heroic days”. Although, it might seem to some as an unpopular field of engineering, this astonishing discipline of Materials Science has been and will continue to be one of the essential subjects for the continuous development and a Brobdingnagian technological advancement mankind would ever witness.

I extend my sincerest gratitude to:

Dr. Balaji Sitharaman for being a professor and mentor and sharing his passion for Carbon nanomaterials. I am indeed thankful to you for making me a member of your research group and giving me the opportunity to explore this field of science. You guided me to pursue my interest through sheer hard work and motivation. Through rough patches and suaveness along the research path, your timely help and counseling was of great assistance.

Dr. Dilip Gersappe for being the respectable and greatly knowledgeable Graduate Program Director. Thank you for enabling me to explore my research interest in carbon nanomaterials by allowing me to work with research group, outside the Department of Materials Science and Engineering. I will always be grateful for your time, advice and suggestions and for the easy-to-approach person that you are.

Dr. Perena Gouma for being an excellent professor and advisor whose lectures kindled my interest in the field of microscopy. Your project assignments and home works definitely helped me mold my research analytical skills.

Dr. Miriam Rafailovich for being a research advisor and a person of immense passion for research. You were one of the many reasons that drove me to pursue a research in Material Science and finally work towards writing a thesis.

Dr. Terry Button for his time, help and suggestions with the CT Phantoms for our project. Without your help it would have been impossible for me and my team members to complete this project

Dr. Jim Quinn for his help and assistance with the SEM and X-ray analysis. Your knowledge, expertise and advices were simply an inspiration. Every moment I spent with you in the Material characterization laboratory, I know for sure I learned something new.

Kenneth James Schaeffer for being a great project partner whose support, ideas, and suggestions helped me from the beginning and I learned a great deal about team work. I will always remember the one sacred quote you showed me, by Richard Feynman, which inadvertently became my stirring inspiration throughout the project. “You can know the name of a bird in all the languages of the world, but when you're finished, you'll know absolutely nothing whatever about the bird. So let's look at the bird and see what it is doing; that's what counts. I learned very early the difference between knowing the name of something and knowing something”.

Juee Vinayak and Debby Michienzi for exceeding my expectations with their support throughout my Master's thesis project.

Galbraith Laboratories and its scientific staff for their assistance with analytical material testing.

Graduate Students Sayan Chowdhury, for help and continual support that gave me a firm start with this research project. Gaurav Lalwani for all his help mainly with the TEM at BNL among others. Shruthi Kanakia for her support and help with the TGA at the last minute. Lab members Dr. Pramod Avti, Dr. Jimmy Toussaint, Sunny Patel, Behzad Farshid, Kelechi Nwachukwu, Jason Rashkow, Yahfi Talukdar, Stephen Lee and others for their support. Graduate students Matt Ferrari, Suphanee, Kai Yang for their precious time and help with material characterization equipment.

All my friends and collegues. Manideep Chavali for his encouragement that motivated me in many situations. Every piece of advice you ever gave with my research work always made me realize, a small bump on the road is never the end of the road itself.

Anuradha Shrimali, for your genuine kindness, generosity, patience, affection and positive reinforcements at times I most needed. I could have never continued to work my way through the semesters without your support and I will always be indebted to you for the perennial support and fillip you continue to show.

My loving family:

Uncle Gideon for his incomparable affection and help beyond any education, Aunt Shanthi, cousins Divya and Arunodhaya whose loving kindness and prayers remained a true motivation throughout my two year degree.

My beloved grandparents Jeevarathinam and Ranjitham, whose wisdom and unconditional love inspired great many things in me. Thank you for leaving a legacy beyond comparison.

Aunt Roseline for her loving encouragement and ever so prayerful wishes. You were and will always be my first teacher and my inspiration for perfection and sincerity at anything I do.

My little sister, Tina for her love and prayers. You inspire me in more ways than you really know. Thank you for being the first best friend and the person whom I have known and grown to admire for your unfaltering affection and hard work.

My parents, Jeyamani and Sundararaj, the only people that are part of any accomplishment in my life. You allowed me to choose the career path I wanted. You led by example in every single step of life. Your unmatched patience, understanding, continuous prayers, steadfast love and timely advices and many other things I can never imagine, continue to mold me to be the person that will definitely make you proud.

Above all, none of this would be possible without Your magnanimous grace, blessings and invisible guidance, my dear Lord. Thank you for all the wonderful people you filled my life with.

Chapter I

INTRODUCTION

I.1 Introduction: Biomaterials

An extensive range of nanomaterials have been engineered, fabricated and characterized for innumerable electrical, mechanical and biological applications recent years. Late advancements in the field of Biomaterial research have shown the development of new types of contrast agents (CAs) for medical imaging applications, using a variety of nanoparticles ranging from Gold to Carbon. Carbon Nanotubes (CNTs) remain the researcher's favorite nanomaterial because of the abundance of properties that can be refined and fine-tuned targeting specific areas of interest. The fabrication of these contrast agents focused mainly on the encapsulation of the medically practicable radiotherapeutic materials like Gold, Silver, Barium, Iodine, Manganese, and so on for corresponding Computed Tomographic (CT) Imaging or Magnetic Resonance Imaging (MRI) applications.

Graphene nanomaterial, a single layer form of Graphite, has proven to have great potential in the area of biomedicine. Currently, Iodine based X-ray contrast agents are the commonest and most widely approved class of radiocontrast agents for CT imaging. We hypothesized the fabrication and development of a new class of Iodinated X-ray contrast agents using Graphene Nanoplatelets (GNPs). This research project presents the synthesis, spectroscopic characterization and analysis of Iodine incorporated Graphene Nanoplatelets through chemical reduction of Graphene Oxide (GO) for use as Computed Tomographic X-ray contrast agents.

Our research involves two major steps in fabricating the Iodine laden Graphene Nanoplatelets. The first step is the synthesis of Graphene Oxide (GO) using the widely acknowledged 'Hummers Method of Oxidation'[1] which involves oxidative treatment of Graphite flakes. Graphene Oxide thus obtained is hydrophilic and thermally unstable due to the

presence of oxygen functionalities. In order to restitute electrical conductivity of Graphene Oxide on par with that of Graphite, a chemical reduction reaction is carried out. Hydrazine Hydrate [2] (N_2H_4) is a conventionally used chemical reducing agent among other effective reducing agents such as Sodium Borohydride [3] ($NaBH_4$). In our research, we hypothesized that the substitution of Hydrogen Iodide or Hydriodic Acid (HI) in place of the toxic Hydrazine Hydrate for the chemical reduction of exfoliated Graphene Oxide could be used to obtain reduced Graphene Oxide Nano platelets. Scanning Electron Microscope and Transmission Electron Microscope images of the Hydrogen Iodide reduced GNPs showed aggregates of platelets and individual nanoplatelets respectively. Energy Dispersive X-Ray (EDX) spectra in correspondence with SEM/EDS and TEM/EDS showed the presence of Iodine at energy level 3.9KeV. The difference in EDS peaks for the oxygen functionalities between Graphene Oxide and HI reduced Graphene Nano Platelets further confirmed the reduction or removal of oxygen from exfoliated Graphene Oxide. Raman spectra for reduced GNPs showed the increase in ratio of D and G band intensities from that of oxidized graphite. Raman Spectroscopy and XRD have been used to further prove the reduction of GO and characterize the Iodine laden nanoplatelets. Computed Tomography Phantoms have been used to study the contrast density of the Iodinated GNPs to confirm the hypothesis that this material can be a prospective x-ray contrast media.

The Iodinated GNPs that were synthesized and characterized during this research, stands out as a significant initiatory step toward the development of Graphene nanoplatelets based CT contrast agent. Over the course of these experiments, we also introduced a novel method for the chemical reduction of exfoliated Graphene Oxide using varying concentrations of Hydroiodic Acid (Hydrogen Iodide). These reduced Graphene Oxide sheets are proven to exhibit electrical

conductivity as compared to Graphite and pave the way for interesting research in the field of Materials Science and Engineering.

I.2 Carbon nanomaterials and their biomedical applications

Carbon Nanomaterials have been in scientists' spotlight for nearly five decades. Carbon nanomaterials continue to find applications in the areas of electronics, micromechanics, energy, Nano composites, and biomedicine and so on. Fullerenes, Carbon nanotubes and Graphene comprise an exceptional class of Carbon-based nanomaterials all of which possess sp^2 chemical bonding [4, 5] enabling them to stand apart from their counterparts.

I.2.1 Graphene

Graphene, since its discovery in 2004 [6] has continued to gain significance owing to its extremely attractive characteristics. In simple words, graphene can be described as a two dimensional single or multi layered sheet of carbon atoms with sp^2 bonding configurations. The synthesis, properties and the extensive feasibilities for chemical alteration of the carbon structure [7] of graphene has made way for potential bio medical applications in a rather cost-effective fashion.

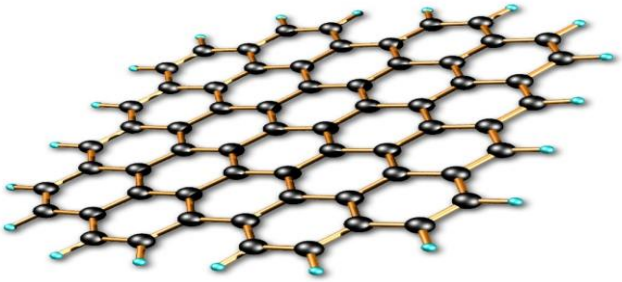

Figure 1.1 2-dimensional illustrative view of single layer Graphene showing hexagonal arrangement of carbon atoms. Source: Lawrence Berkeley National Laboratory.

I.2.2 Graphene and Carbon nanotubes

Carbon nanotubes (CNTs), being the most specialized variety among closed graphitic structures possessed distinctive mechanical strength, electrical and thermal conductivity characteristics. Shortly after their discovery in 1991 [8], CNTs became a rapidly emerging subject in research and have shown applications in drug delivery, gene delivery, biosensors and medical imaging. Graphene, on the other hand, being the younger and yet-to-mature member of the same family as CNTs, do not possess the same optical properties and hence posed limitations in photothermal and photoacoustic imaging. However, when reduced graphene oxide was used, it was shown to have better *in vitro* photothermal responsiveness than that of CNTs. Also, the cost of mass synthesis of Graphene Oxide is many fold lesser than that of CNTs which still seem to be an expensive material [9].

I.2.3 Graphene Oxide

Graphene Oxide was first prepared in 1850 by using Potassium Chlorate and Nitric acid as oxidizing agents by Brodie et al. Since then, there have been many different variations in the preparation of Graphene Oxide. However, it was William Hummer in 1958 who prepared Graphene Oxide by the oxidation of Graphite flakes using potassium permanganate, a very common oxidizing agent, followed by a treatment with Sulphuric acid and Nitric Acid combination [1]. It would be appropriate to say that Graphene Oxide is much similar to Graphite Oxide chemically. However, in the structural sense these two materials differ in the fact that Graphene oxide has an exfoliated appearance with well-spaced single layers or scarcely stacked layers and does not possess the heavy stacked layer structure of Graphite Oxide [10].

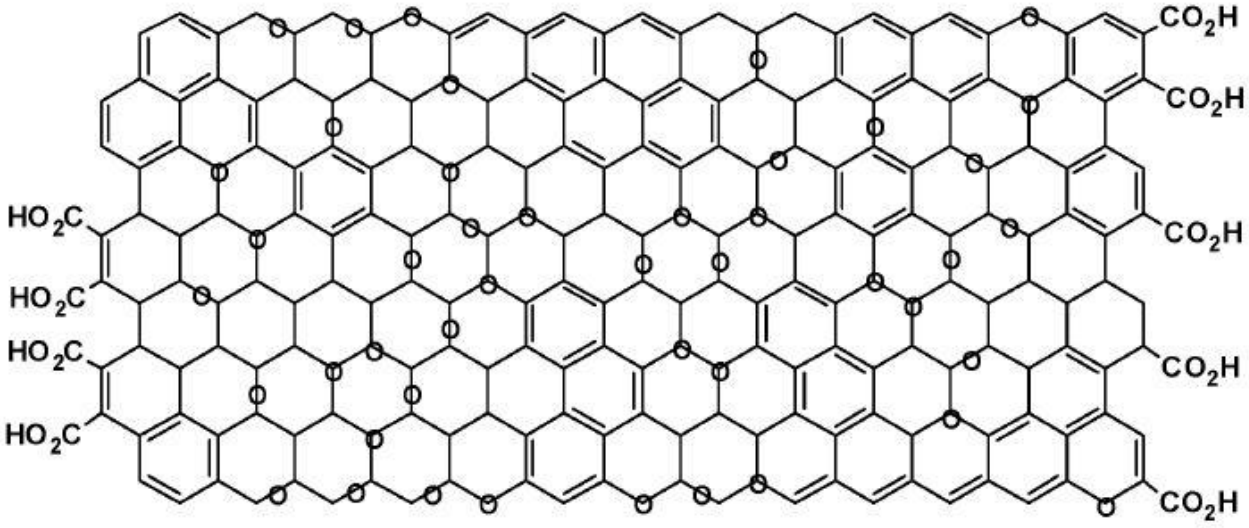

Figure 1.2 Structural model of Graphene Oxide. Reprinted from literature [10]

I.3 Chemical reduction of Graphene Oxide

Graphene oxide is chemically modified (oxidized) graphite and by itself does not show any electrical conductivity. Graphitic oxide consists of multi layered sheets of oxidized graphene and each sheet consisted mostly of epoxide and hydroxyl groups [11]. In order to bestow the conductivity in exfoliated graphene oxide, it had to be stripped off the oxygen functionalities that make them highly hydrophilic allowing intercalation of water molecules. In other words, Graphene Oxide has highly disoriented sp^2 bonding due to the presence of oxygen atoms that randomly bond to graphene sites and convert them to sp^3 carbon bonds eventually making them electrically insulative [12, 13]. So, in order to render them with properties similar to those of Graphite, the sp^2 configurations have to be restored.

A number of different techniques have been proposed for the reduction of graphene oxide. Chemical reagents that have been used to reduce graphene oxide include, but are not

limited to, Hydrogen Sulphide, Hydrazine Monohydrate, Sodium Borohydride, Hydroxylamine, Dimethyl Hydrazine, Hydroquinone, NaBH4 in combination with Sulphuric acid, Aluminium powder, Benzylamine and even urea as an expansion-reduction agent [14-23].

Among all the above mentioned reducing agents, Hydrazine Hydrate was and still is the commonly used reagent to achieve a significant reduction. Even though there were no confirmed reaction paths for the action of Hydrazine on Graphene Oxide, Stankovich et al showed a proposed mechanism of the reduction, as seen in Scheme 1.

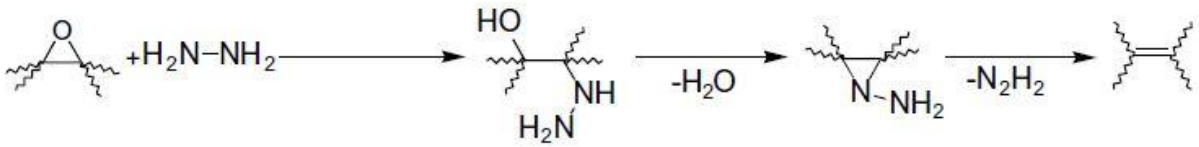

Scheme 1.1. Proposed epoxide reduction reaction mechanism using Hydrazine Hydrate (N_2H_4). Reprinted from literature [2]

In this research, we embarked on a new attempt to use a chemical reducing agent that was strong enough to reduce the Graphene Oxide and at the same time would incorporate Iodine into the graphene layers in order for it to be developed into a potential X-ray contrast agent. Following the same reaction route of GO reduction using N_2H_4, we hypothesized that Hydrogen Iodide (or Hydroiodic acid) would accomplish our mission.

I.4 Hydrogen Iodide

Hydrogen Iodide is a diatomic molecule that comprises of one Hydrogen atom and one Iodine atom. Technically, Hydrogen Iodide is produced by replacing one Iodine atom in Iodine molecule (I_2), with one Hydrogen atom. Hydrogen Iodide is readily soluble in water contrary to Iodine which hardly has any water solubility. Hydroiodic Acid is prepared by the dissolution of Hydrogen Iodide in water.

Hydroiodic Acid (HI) is a strong acid due to the fact that the bonding electrons from the fifth orbital in Iodine atoms are weakly bonded to the electrons in Hydrogen's first orbital. HI is also a very strong reducing agent and became extremely popular when it was used in combination with red phosphorus, in the synthesis of Methamphetamine through the reduction of Ephedrine [24]. Due to this reason, it is listed as a Federal Drug Enforcement Administration List-I Chemical by the United States Controlled Substances Act, 21 U.S.C. § 802. It is important to mention that, in this research, HI was not used for any illicit purposes or any purposes at all other than the reduction of Graphene Oxide. The storage temperature for Hydroiodic Acid is 2ºC - 8ºC and it was always stored in a refrigerator before and after every use.

I.5 X-ray Contrast media

Contrast agents (CA) or contrast media are, in simple words, substances that help heighten the contrast of any medically significant tissues, organs and that sort. Among various other classifications of contrast agents, the ones that work on the basis of X-ray attenuation are called X-ray contrast agents. Barium and Iodine are to this the date the most commonly used mediums for X-ray contrast agents.

Iodinated contrast media has undergone several significant improvements in various aspects of their development with importance mainly given to the minimization of risks associated with intravascular contrast agents. Most iodinated intravascular Contrast Agents have tri-iodo-benzene type of structural formulation. These are further classified into other types based on their physicochemical properties, ionic or nonionic, osmolality, percentage or concentration of Iodine and so on. In our research we tried to show that Iodine bonded to Graphitic structures can prove to be potential contrast agents for Computer Tomographic Imaging and would pave the way for many other related applications. Iodine concentration of an X-ray contrast agent signifies how effective the X-ray attenuation of material would be. The possibility of absorption of higher X-ray photons for better contrast is directly proportional to the concentration of Iodine (radio-opaque material) in the CA.

Concurrently, it is extremely important to understand the fact that the risk and fatality of adverse side effects and reactions due to intra vascular injection of CAs increases with the increase in Iodine concentration. This makes it essential for scientists to develop a contrast media that will possess the best of both characteristics by incorporating the optimum amount of Iodine to achieve the necessary contrast and not compromise the patient's health.

I.6 Computed Tomography Imaging

X-ray Computed Tomography commonly referred to as Computed Tomography (CT scan) or Computed Axial Tomography (CAT scan) is a diagnosing tool which utilizes image sectioning tomographic principles and finds extensive applications in medical centers and industries. The construction of the scanner is such that, the X-ray source that moves around the subject under study and opposite the x-ray source is the detectors. X-Ray slice data is generated

by rotating the source around the object while the detectors measure the intensity of the exiting beam which in turn is directly related to the radio density of the subject under study. The images obtained can be reconstructed as desired using the computer in to a 3D image. This being the basic working principle of the CT scan, while scanning the human body that has different organs and tissues with different radio densities, the necessity of a contrast agent arises. The uses of CT include a wide variety of disease diagnosis and continuous research is being carried out to further improve the range of applications in health care and medicine.

I.7 Characterization Techniques

Most of our research concentrated on the analysis and characterization of materials that have been synthesized and fabricated. Hence it was important to carefully choose the types of material characterization techniques to be used in order to obtain and analyze the results. Spectroscopic characterization techniques played an immense role in studying the materials and greatly assisted in analyzing the results both quantitatively and qualitatively. Since this was a research project that was solely improvised based on extensive literary surveys and hypothesis, it was important to carry out as many characterization techniques possible and available in order to achieve convincing results. Elemental analysis of the synthesized material was the foremost requirement since sizable evidence to confirm the presence of Iodine was needed. Identifying the iodine in the Hydroiodic Acid reduced graphene oxide to figure out in which chemical states it existed inside the graphene nanomaterial or if it existed as free iodine ions or if it existed at all was a slightly larger job than it appeared to be.

I.8 Materials and Methods

The following solvents and reagents were of ACS reagent grade or better and were used as was, without any further physical or chemical modification.

Graphite powder	<45 μm, ≥99.99% Sigma-Aldrich
Formic Acid(H-COOH)	puriss. p.a. , ~98% (T) Sigma-Aldrich
Potassium permanganate ($KMnO_4$)	ACS reagent, ≥99.0% Sigma-Aldrich
Hydrazine Hydrate solution ($H_2N=NH_2$)	puriss. p.a. 24-26% in H2O Sigma-Aldrich
Hydroiodic Acid (HI)	57 wt. % in H2O, 99.95% Sigma-Aldrich
Methanol (CH_3OH)	99.9% HPLC-UV grade Pharmo-Aaper
Sulphuric Acid (H_2SO_4)	98.0% USP/NF grade J.T Baker
Nitric Acid (HNO_3)	69.0 - 70.0 % USP/NF grade J.T Baker
Acetone ($CH_3C=OCH_3$)	99.5 % USP/NF grade J.T Baker
Dextran	Technical grade powder. T_6- 6000Da; T_{10}-10000Da Pharmacosmos A/S, Denmark

Scanning Electron Microscopy was performed on all samples using the LEO 1550. The LEO 1550 was an ultra-high resolution field emission SEM utilizing the GEMINI field emission column. It had a Cartesian stage with motorized axes, superb resolution at low operating voltages and short working distance of 8.5 mm for simultaneous high resolution SE or BSD imaging. With an accelerating voltage of 200V to 30kV, the LEO 1550 was able to acquire images using an In-lens annular detector, a secondary electron detector and a backscattered electron detector.

Transmission Electron Microscopy was performed at the Central Microscopy Imaging Center in the Life Sciences Department at Stony Brook University using a FEI BioTwinG^2 Transmission Electron Microscope. The BioTwonG^2 was equipped with an AMT digital camera for acquiring images as well as film capability. It functioned at an accelerating voltage of 120kV with goniometer/stage tilt capability and it utilized software for serial reconstruction.

High Resolution Transmission Electron Microscopy was performed using the JEOL 2100F HR-TEM at the Institute for Advanced Electron Microscopy in the Center for Functional Nanomaterials at Brookhaven National Laboratory. The JEM-2100F is an advanced Field Emission Electron Microscope featuring ultrahigh resolution and rapid data acquisition. It has one of the highest analytical performances in the 200kV class analytical TEM with a probe size under 0.5nm and can also be equipped with STEM, MDS, EDS, EELS, and CCD-cameras

Energy Dispersive X-ray was performed on dry bulk powder samples in order to obtain information about the chemical composition of the materials that were tested. The EDS attached to the LEO 1550 SEM had a high probe current than 0.5% per hour for fast X-ray analysis and EBSP pattern acquisition. The SEM/EDS was the first technique that was used to identify the materials present in the HI reduced graphene oxide, Hydrazine reduced platelets, Graphite and Graphene oxide allowing a comparative analysis. There was another EDS used and was a part of

the TEM and also provided information on the chemical composition of the HI reduced nanoplatelets.

Raman Spectroscopy was performed using Enwave Pro-Raman. It used a 785nm frequency stabilized narrow line width diode excitation laser with shutter control. The CCD detector was cooled to -60 degree Celsius and approximately a standard working distance of 7mm was used. The software used to obtain and analyze the spectra was supplied by Enwave Optronics for Time Chart & Time Trend for real time reaction monitoring and also enabled us to use single scan and continuous scan modes as required.

Micro Raman with Scanning Probe Microscope was performed using the WI Tec alpha300R Micro-Imaging Raman Spectrometer in the Department of Geosciences at Stony Brook University. The WI Tec alpha300R confocal Raman imaging system was equipped with both 532 nm Nd YAG and 325 nm HeCd excitation lasers. A variety of objective lenses provided white light and Raman imaging capability at scales ranging from 260 nm/pixel to several μm/pixel. Two holographic grating spectrometers allowed the collection of Raman spectra at 3 cm-1 or 1 cm-1 spectral resolution over a wide Δcm-1 range.

Ion specific electrode measurement was performed following the oxidative combustion at Galbraith Laboratories, Tennessee. Ion specific/selective measurement basically works under the principle in which an ion selective electrode which in turn is a transducer that is capable of converting the activity of specific ion under study, into an electric potential that can be measured using a voltmeter. *Oxidative Combustion* or *Oxidative Flask Combustion* was performed by the scientific staff at Galbraith Laboratories using an Erlenmeyer flask (oxygen flask). Combustion aids were added as necessary and a known volume of absorbing solution was added to the oxygen flask. The flask was purged at atmospheric pressure with oxygen. The flag containing the

sample was then ignited and immediately sealed into the flask using a silicone rubber stopper fitted with a solid quart rod. Once combustion was complete, the flask was inverted several times to effect quantitative absorption of the liberated gases. This oxygen flask combustion method was primarily used for the detection of Halogens. The protocols for oxidative combustion and the ion selective electrode measurement were provided by Pat DeLozier of Galbraith Laboratories and were based on the references from the American Society for Testing and Materials, ASTM E-442, Test Method for Chlorine, Bromine, or Iodine in Organic Compounds by Oxygen Flask Combustion.

X-Ray Diffraction was performed on a Philips Analytical X-ray detector in the Department of Materials Science and Engineering, Stony Brook University. XPLOT for Windows, an IBM PC based program for the manipulation of step or continuous scan X-ray diffraction patterns was used. The program is primarily designed to display the X-ray data in a convenient graphical form and allow features of the patterns to be examined in detail. There were facilities within the program for automated and manual peak location, pattern addition (or subtraction), and computer Search/Match of the measured pattern using data from the ICDD CD-ROM database (license from ICDD). The software that was used to acquire the actual X-Ray diffraction pattern was the PC-1710. Both these software were from CSIRO Land and Water. Powder-X software was also used as and when necessary for subtracting the background and smoothing the spectral data.

CT Phantoms were performed using GE Light Speed VCT at the Department of radiology, Stony Brook University Hospital and the Cancer Center, Stony Brook University through the kind favor of Dr. Terry Button, Director of Medical Imaging Technology program in the School of Health Technology and Management.

All centrifugations were done using the SORVALL RT7 Tabletop Centrifuge from Kendro Laboratory products at the Department of Biomedical Engineering, Stony Brook University. The SORVALL RT7 was equipped with a refrigerator system, a low temperature condensing unit, a closed loop speed control and also an optional tachometer port that allowed calibration. The centrifuge had a temperature range of -5º C to +25º C, a temperature accuracy of ±2º C, a maximum rotor speed of 7000rpm. Spin Coating of samples was performed using the WS-650 Lite Series spin processor from Laurell technologies. The WS-650-series coater system accommodated up to ø150mm wafers and 5" × 5" (127mm × 127mm) substrates, and also featured a maximum rotational speed of 12,000 RPM (based on a ø100mm silicon wafer). However, we used only a maximum of 4000rpm for our purposes. Spin coated samples were used for SEM and AFM imaging

Chapter II

Synthesis Efforts Toward Iodine Laden Graphene Nanoplatelets

Results and Discussion

II.1 Synthesis of Graphene Oxide

The synthesis of Graphene Oxide involves a pre-oxidation step and an oxidation step followed by dialysis and drying. This solution based method of producing graphene nanosheets has been a proven technique for the production of large quantities using a relatively simple procedure [25].

II.1.1 Pre-oxidation

In a typical experimental routine, during the pre-oxidation step, 2g of Graphite flakes were treated with about 50ml of Formic Acid in a round bottom flask and the mixture was ultrasonicated for 2 hours at room temperature conditions. The resulting dispersion is transferred to falcon tubes and is centrifuged thrice for 20 minutes and 3000rpm each at room temperature. The first centrifuge is simply to remove the formic acid followed by washes with de-ionized water (DI-water) and acetone respectively. At the end of this procedure, Graphite flakes are exfoliated in to Graphite Nano Platelets and are dried in a vacuum oven for 12 hours at about 65 degree Celsius.

It was important that the pre-oxidation step be carried out before the actual Hummer's method of oxidation was to prevent the occurrence of any graphite core particles due to partial oxidation. It also plays a crucial role by stepping up the overall efficiency of oxidation by increasing the surface area of the particles [26].

II.1.2 *modified* - Hummers method of Oxidation

The graphite nanoplatelets thus obtained after the pre-oxidation and drying steps was then transferred to a round-bottomed flask placed in an ice cold bath. 20ml of 70% Nitric acid was

added slowly into the flask and was mixed well using a magnetic stirrer for about 1 hour. The stirring was stopped and 30ml of 95% Sulphuric acid was added gradually to avoid the effervescence while the flask was still maintained in the ice bath. Following this, 6g of 99% Potassium Permanganate was added carefully into the mixture. The mixture was kept in the ice bath until all increases in temperature due to the addition of acids were normalized. After a few minutes, the flask was removed from the bath and placed in an oil bath at 35 degree Celsius and mixture was stirred magnetically for 2 hours. At the end of 2 hours, 200 ml of DI water was added and the mixture was continued to stir until a dark brown colloidal suspension was obtained. The suspension was then stopped heating and allowed to stir and cool down for 30 minutes following which it was centrifuged at 3000rpm for 20 minutes. The supernatant obtained after the wash was discarded. The resulting particles were repeatedly washed using DI water several times and subject to dialysis for further removal of free ions for three days. Dialyzed graphite oxide nanoplatelets were then dried for a week in a desiccator under vacuum, over phosphorus pentoxide to remove all moisture. At the end of seven days, the dry powder was collected and stored.

It is to be noted that during this modified Hummer's method of oxidation, the Graphite nanoplatelets undergo a broad change in their structure. The overall concentration of oxygen in the particles increases with simultaneous slight reduction in the carbon content which eventually increases the oxygen-carbon (O/C) ratio [26]. A breakage of the carbon sigma bonds to form sp^3 bonding structure is observed during this process of oxidation where oxygenated carboxyl and epoxide groups are generated [26].

II.2 Reduction of Graphene Oxide

As discussed earlier in this paper, the main purpose for the reduction of graphene oxide was to restore its characteristics close to that of graphite. Graphite with its sp^2 structure is highly hydrophobic, whereas when oxidized these characteristics are lost completely. Figure 2.2 shows the high water solubility of graphene oxide compared to graphite. Graphite settles down to the bottom of the glass vial in less than 10 minutes, whereas the changes in bond configurations in GO allow water intercalation making them highly hydrophilic.

(a) 

(b) 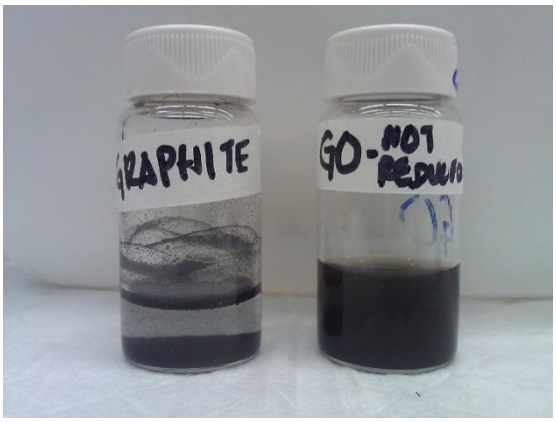

Figure 2.1 Photograph of (a) Graphite and GO in water (b) Graphite and GO in water after 10 minutes; high water solubility of Graphene oxide

There have been numerous methods for the chemical reduction of graphene oxide among other mechanical and thermal routes. However, in this research thesis we hypothesized the reduction of Graphene Oxide using a strong acid and a reducing agent like Hydroiodic Acid (Hydrogen Iodide). However, it was important to understand the concentration of HI that would bring about a complete reduction and also at the same time incorporate Iodine into the graphitic structure. The percentage yield of the reduced graphene oxide was also taken in consideration while carrying out the reduction.

II.2.1 Reduction of GO using Hydrazine Hydrate ($H_2N=NH_2$)

Stankovich et al. had used Hydrazine Hydrate to chemically reduce exfoliated graphene oxide. We used similar concentrations of Hydrazine Hydrate to reduce the GO that was synthesized using Hummers method. Although, it might or might not be influencing the structural change occurring in reduced Graphene Oxide, it could be practicable to know that the structure of Hydrazine has sp^3 hybridized nitrogen atoms.

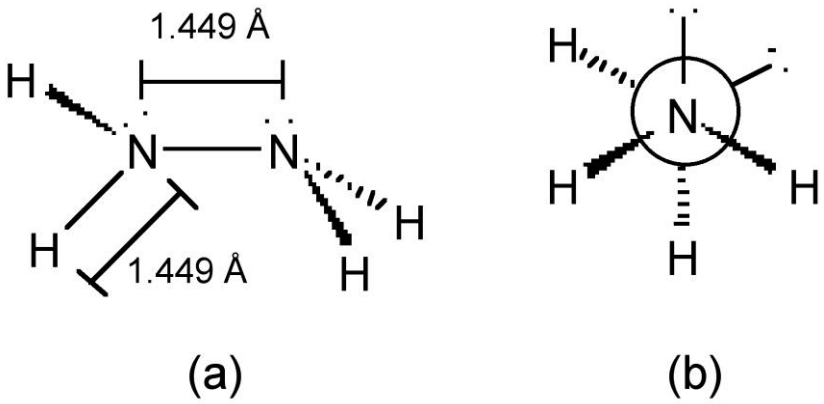

Figure 2.2 The structure of Hydrazine Hydrate. Source: Andrew R. Barron, *The Connexions Project*

In a typical chemical reduction of GO, we used the 24-26% Hydrazine Hydrate solution obtained from Sigma-Aldrich. 150mg of dried Graphene Oxide powder was taken in a 500ml round bottomed flask and 150ml of DI water was added to it. The mixture was ultrasonicated for about 1 hour and it was made sure there was complete dispersion of GO in water. The flask was then placed in an oil bath at 95 degree Celsius. To the 150ml dispersion 32.1mM (1.5ml) concentration of Hydrazine Hydrate solution was added and continuously stirred using a magnetic stirrer. The top of the flask was connected to a water condenser that circulated ice cold water from an ice bath, the temperature of which was maintained constant. The setup was not

disturbed and the reaction was allowed to proceed for 24 hours and then the heating was stopped. The flask was then removed from the oil bath and allowed to cool under room temperature for 30 minutes. After cooling, the mixture was then centrifuged to discard the supernatant. It was washed twice with water and once with methanol respectively before placing inside a vacuum oven at 65 degree Celsius. After drying overnight, the powder was collected and stored.

II.2.2 Reduction of GO with Hydroiodic Acid

We compared the reduction of GO using HI to that of the reduction of GO using Hydrazine. Chemically, HI consists of Hydrogen H^+ and Iodine in its lower oxidation state as I^-. This allows HI to act readily as a reducing agent since it is able to provide electrons for the reduction of a material by getting easily oxidized itself due to the weak H-I bond.

Initially, varying concentrations of Hydroiodic acid was used to chemically reduce the GO and study the difference in their characteristics. The first experiment was run using 8.025mM concentration of HI. 50mg of exfoliated GO was dispersed in 50ml of DI water and was ultrasonicated in a round bottomed flask to obtain a complete and uniform dispersion. The flask was then placed in an oil bath maintained at 80-85 degree Celsius. 8.025mM concentration of HI was added to the dispersion placed in the oil bath and was constantly stirred using a magnetic stirrer. The top of the flask was connected to a water condenser that circulated ice cold water to keep the reaction temperature under control and also to condense any evaporated liquid from the flask. The water cooled condenser helped in retaining the volume of the dispersion. The setup was not disturbed for 24 hours and the reaction was allowed to complete. The temperature of the ice bath was maintained constant.

At the end of the reaction, the heating and stirring were stopped and the dispersion was allowed to cool for about 30 minutes. Later the mixture was transferred carefully into falcon tubes for centrifugation. The supernatant was cautiously discarded without losing any particles. The particles were washed twice with DI water and once with methanol before placing them in the vacuum oven at 65 degree Celsius. After drying overnight, the powder was collected, weighed and stored. The percentage of yield was calculated and recorded.

Using the similar protocol, the HI reduction of Graphene Oxide was carried out with varying concentrations of HI such as 8.025mM, 16.05mM, 23.45mM and 32.1mM in order to analyze and study the differences in the reduction efficiency, yield, amount of Iodine incorporated and so on. It was made sure that the Graphene Oxide batches that were reduced using different HI concentrations were all from the same batch of synthesis, in order to expect consistency in the results.

II.2.3 Chemical Waste Disposal

The reagents that were used during the synthesis of graphene oxide and the following reduction reactions are toxic, corrosive and hazardous. Waste from the synthesis of graphene oxide contained mixture of concentrated Sulphuric acid, Nitric acid and Potassium permanganate. They were disposed carefully after dilution with excess of DI water and were not mixed with any other chemicals or reagents. Hydrazine Hydrate waste and Hydroiodic Acid waste were also disposed in a similar way in separate waste disposal containers after dilution with excess water.

II.3 Results and Discussion

The first set of characterization techniques that were performed on the samples to study and analyze the properties, morphology and chemical composition. These included SEM/EDX and Raman. Following the confirmation that Iodine was present in these samples the next set of characterization techniques were focused more on narrowing down to which sample type was best suited for developing a potential contrast agent.

II.3.1 Scanning Electron Microscopic Imaging

As mentioned earlier in this thesis, the LEO 1150 Gemini Scanning Electron Microscope with a field emission electron gun was used to obtain microscopic images of the tested material. The regular backscattered electron detector was used and the SEM was operated at a voltage of 20KV. The working distance was mostly not varied and was kept between 10mm to 12mm.

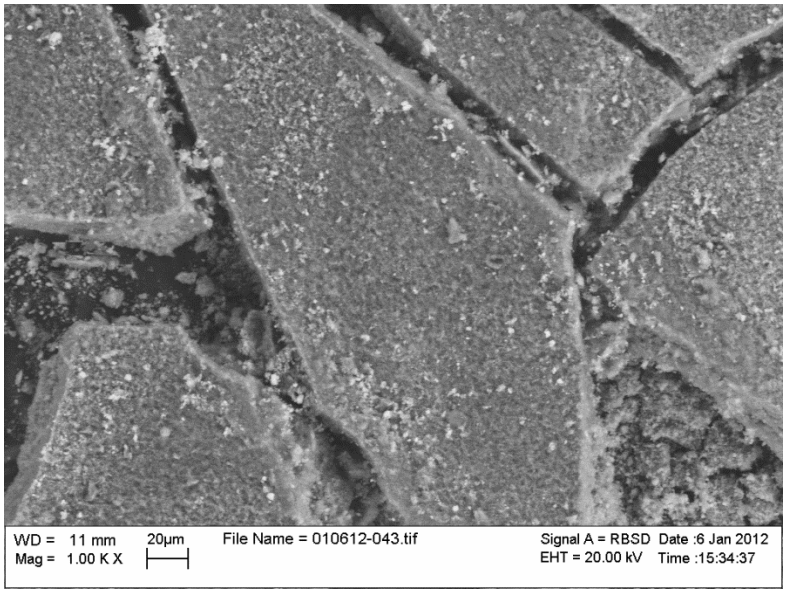

Figure 2.3 SEM Image of Graphene Oxide synthesized through the modified Hummer's method

There were no specific sample preparations needed for the SEM. However, it was important for the sample to show some conductivity. We used bulk dry powder samples and used two sided tapes to retain the sample on the holder. It was also made sure that the samples were all completely dried before any analysis. Figure 2.3 shows the SEM image of Graphene Oxide nano platelets synthesized using the modified Hummers method of oxidation as described earlier. The image shows an aggregate of tightly packed powder of GO.

(a). 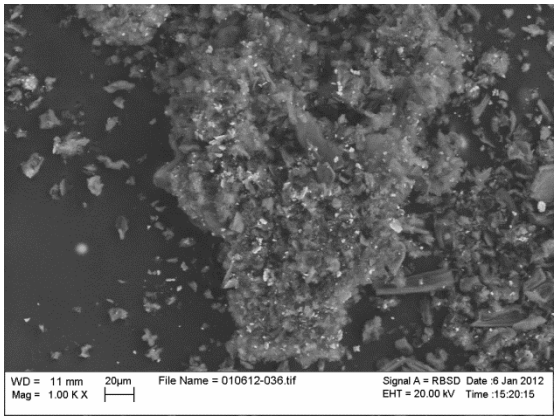

(b). 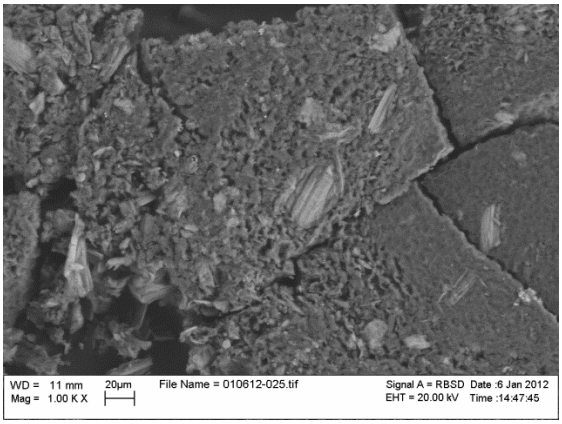

(c). 

(d). 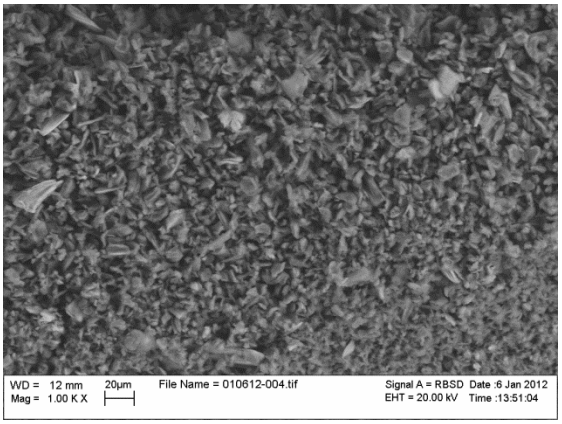

Figure 2.4 SEM Images of (a) N_2H_4 reduced GO (b) 8.025mM HI reduced GO (c) 16.05mM HI reduced GO (d) 32.1mM HI reduced GO

The rugged look is mainly because of the dryness of the sample and also it appeared to stick together like tiny pellets that took the shape of the falcon tubes they were dried in. SEM

images of reduced graphene oxide were also obtained. We used Hydrazine Hydrate as a reducing agent for one batch of samples, to use as a control and three other different concentrations of Hydroiodic Acid reduced GO. All samples looked aggregated due to the fact they were all just bulk dry powder. At higher magnifications, we observed layers of graphene nano sheets clubbed together although. At lower magnification levels, the images mostly showed the general morphology of the material. From figure 2.3 we observed that the general morphology of the Hydrazine reduced GO and HI reduced GO did not show any significantly distinct differences. However, when the samples were spin coated at 2000rpm on a silicon chip before performing SEM, the images obtained differed in many aspects. For all the images showed above, the back scattered electron detector of the SEM was used.

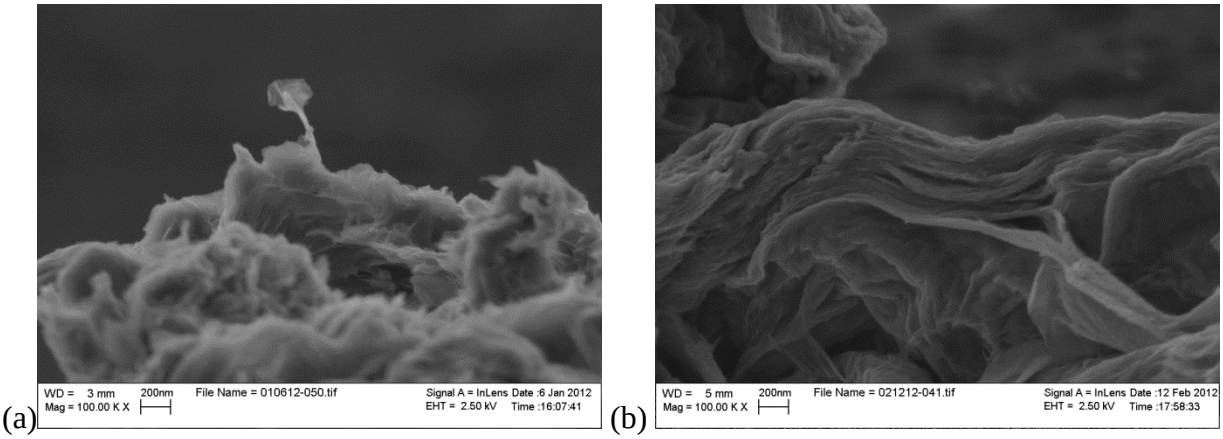

Figure 2.5 (a) 32.1mM HI reduced GNP –powder sample (b) 32.1mM HI reduced spin coated sample showing stacked layers

When the In-lens and Secondary electron detectors were used, we obtained images showing the stacking of graphene layers and aggregates of graphene nanoplatelets. In figures 2.5 (a) and 2.5 (b)we can observe the stacked and tightly packed layers of HI reduced graphene nanoplatelets. However, using the In-lens detector to obtain the images resulted in a slightly

different image quality and inadequate contrast which might be because of fewer electrons scattered in the direction of the detector. Altogether, from the SEM images we were able to look into the morphology of these platelets comparing them with unreduced graphene oxide and hydrazine reduced graphene oxide.

II.3.2 Transmission Electron Microscopic Imaging (TEM)

The Transmission Electron Microscopy was performed using the FEI BioTwinG2 Transmission Electron Microscope (TEM) at the Central Microscopy Imaging Center in the Life Sciences Department at Stony Brook University. Unlike SEM samples, TEM samples were prepared and strained on a copper grid that was to be placed on the TEM sample holder.

(a)

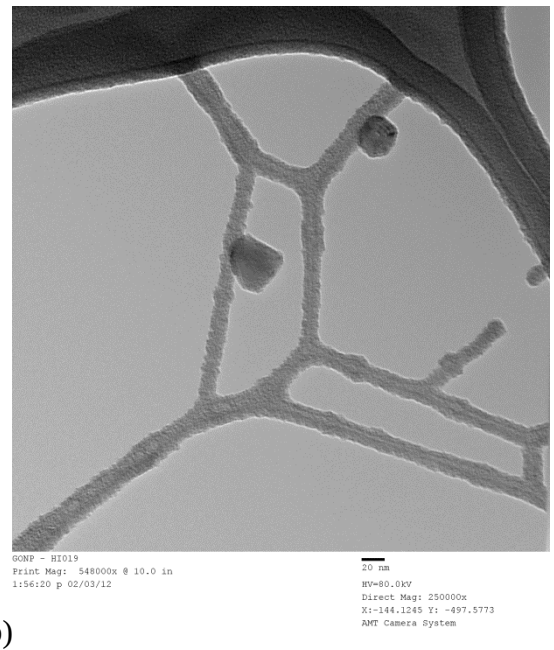

(b)

Figure 2.6 Low resolution TEM images of HI reduced Graphene Nano Platelets at low magnification

The samples were prepared by making a 1mg/ml solution concentration i.e. by dispersing dry powder in a 1:1 methanol and DI water mixture. The dispersion was probe-sonicated on ice

with 1sec ON and 2 sec OFF cycles. When the mixture was completely sonicated to get a uniform dispersion, a drop of the dispersion was placed carefully on the copper grid. The grids with the samples were allowed to dry under room temperature for about 2 hours or overnight. Later the grids were transferred on to the TEM sample holder to obtain images. Since the dispersion was a 1mg/ml concentration it was appropriate not to expect to see many number of platelets at a higher magnification.

In the low resolution TEM we were able to observe the clusters of platelets that seemed to have stacked over one another. Figure 2.6 shows the Low res TEM images of HI 32.1mM HI reduced GNPs. In figure 2.6(a) we see the stacks of graphene nanosheets clubbed together and figure 2.6(b) shows two individual platelets at different locations on the grid. After studying a number of images, the platelets showed to have lengths range of 50nm to 250nm. This seemingly uneven distribution of dimensions of these platelets might not be the actual length of platelets that were synthesized. There was an immense possibility for change in dimensions of the platelets during the sample preparation where they were dispersed in solution following ultrasonication and probe sonication. During these mixing actions, the fine layered platelets would shear against each other and that would have resulted in their stretching and change of dimensions. However, this process cannot be confirmed. Further low res images were also showed the single graphene sheets at different locations on the TEM grid. Figure 2.7 shows single or minimal layers of graphene nano sheets that resemble crispy thin wafers. For this reason, the TEM is better in obtaining images of such better quality than the SEM even though the spin coated samples looked better than bulk dry powder.

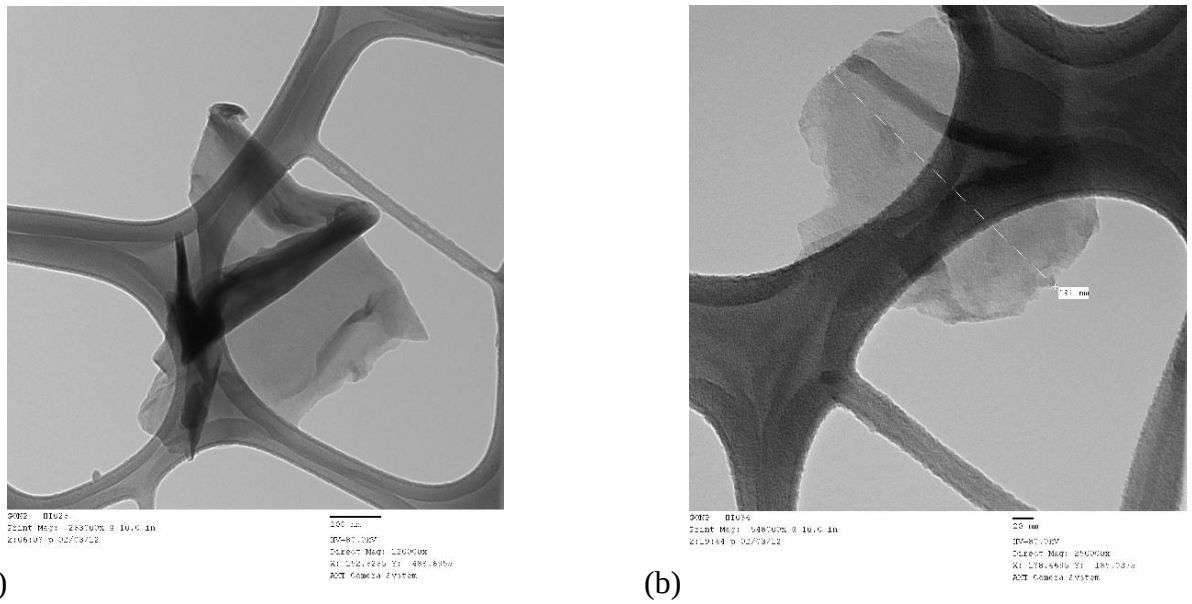

(a) (b)

Figure 2.7 Low resolution TEM images of HI reduced Graphene Nano Platelets at high magnification showing single or few layers of graphene nano sheets

II.3.3 High Resolution - Transmission Electron Microscopic Imaging (HR-TEM)

The high resolution TEM was performed using the JEOL 2100F HR-TEM at the Institute for Advanced Electron Microscopy in the Center for Functional Nanomaterials at Brookhaven National Laboratory. High Res images showed the images aultra high magnification ranging from 10nm to 100nm. Even higher magnification levels showed upto 2nm distance of the samples under study. Figure 2.8(a) and Figure 2.8(b) show High Res TEM images of 32.1mM HI reduced GNPs at the 10nm and 5nm level . The images showed the steps of layered nano sheets one on top of the other. These images were better than those obtained with the SEM and Low Res-TEM. As we know that 1nm = 10 angstroms, from these images at the 5 nm level it is appropriate to interpret them as having 50 angstrom distance. Considering the distance between two carbon atoms in the graphitic structure to be aroun 1.4 angstrom, these HR-TEM images allowed us to see around 35 carbon atoms in the 5nm level. Even further higher magnification

images as shown in figures 2.8(c) and figure 2.8(d) we might be able to see aroun 14 atoms in the 2nm level.

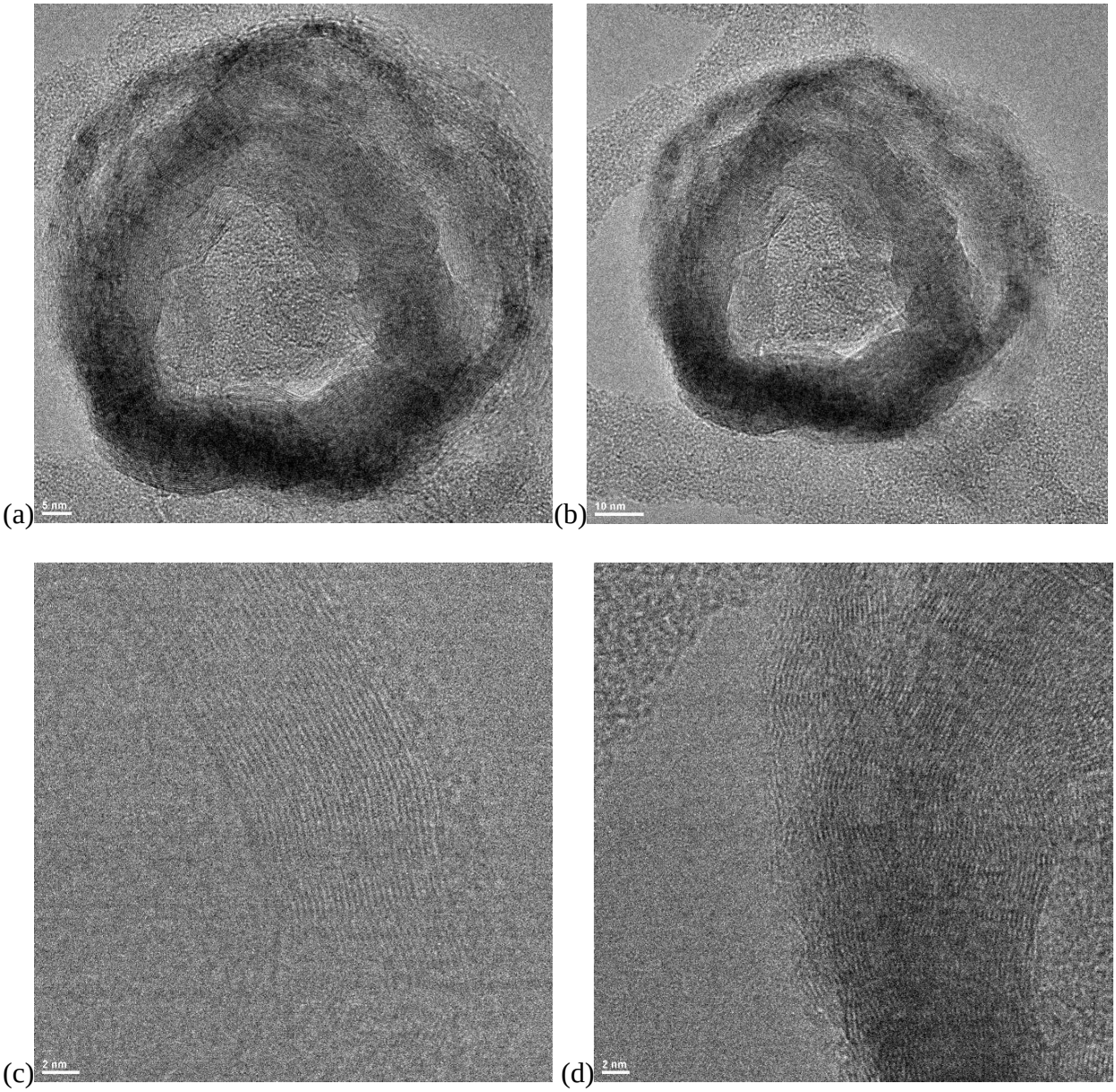

Figure 2.8 High Resolution TEM images of HI reduced Graphene Nano Platelets (a) 5nm level magnification (b) 10nm level magnification (c) and (d) 2nm level magnification

These images gave an interesting set of information about the morphology of graphene oxide, HI reduced platelets and Hydrazine reduced platelet at different magnification levels, their dependance on the ratio of dipersion and other parameters.

II.3.4 Energy Dispersive X-Ray Spectroscopy (EDS/EDX)

The Energy dispersive X-ray Spectra was obtained using two different set of equipment, one that was connected to the LEO 1550 Scanning Electron Microscope and the other with the JEOL 2100F HR-TEM. Both of these instruments were connected with X-Ray microanalytical detectors that detected characteristic X-rays from the sample under study and showed spectra containing information about the chemical composition.

The working principle of X-ray microanalysis is that, when an high energy electron beam hits the sample, the electron(s) in the inner shell are knocked out and the empty spot is immediately filled by the electrons from the outer shell. In this process, the energy equal to the difference in energy between the outer shell (from which the electron was transferred) and the inner shell (to which it was transferred) is emitted as X-Ray. These X-rays are detected by the x-ray detector connected to the SEM or TEM, and since these X-Rays are characteristic of the material they are emitted from, the resulting spectra from the detected waves provide an accurate information about the chemical compostion of the material.

We performed SEM/EDS on Graphene Oxide, Hydrazine reduced platelets and the platelets reduced using different concentrations of Hydrogen Iodide. As showed in figure 2.9, the Energy dispersed spectra of graphene oxide bulk powder confirmed the presence of high amounts of Manganese and also Oxygen explaining the fact that the Hummer's method converted exfoliated graphite into graphene with oxygenated groups. The presence of manganese and potassium peaks were due to the use of Potassium permanganate as oxidising agent. The

small peak showed for copper was because of the copper stubs on to which the powder was taped.

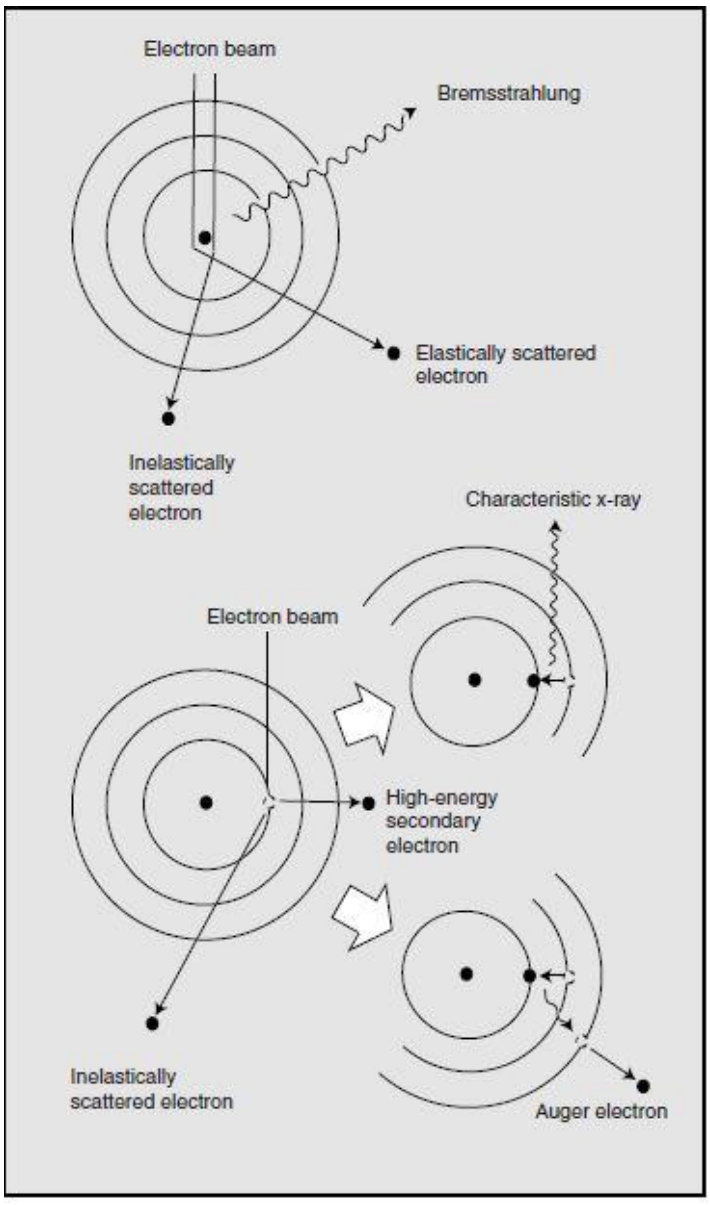

Figure 2.9 Inner shell electron ionization in an atom and subsequent de-excitation by electron transitions. The difference in energy from the electron transition is expressed either as the ejection of an energetic electron with characteristic energy or by the emission of a characteristic X-ray photon. Source: An Introduction to Energy-Dispersive X-Ray Microanalysis, NORMAN Instruments.

(a)

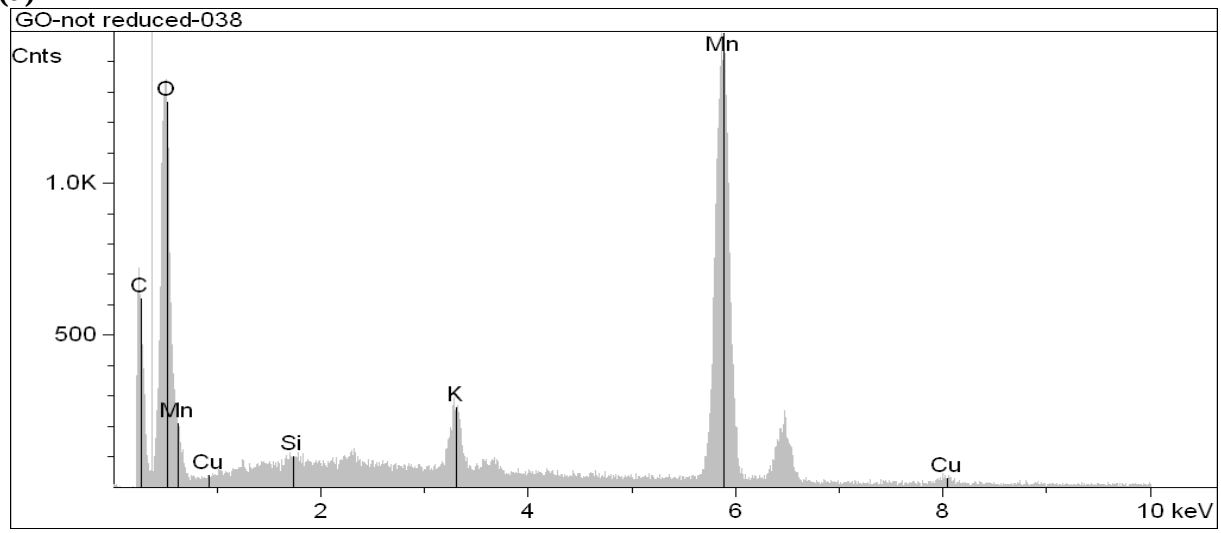

(b)

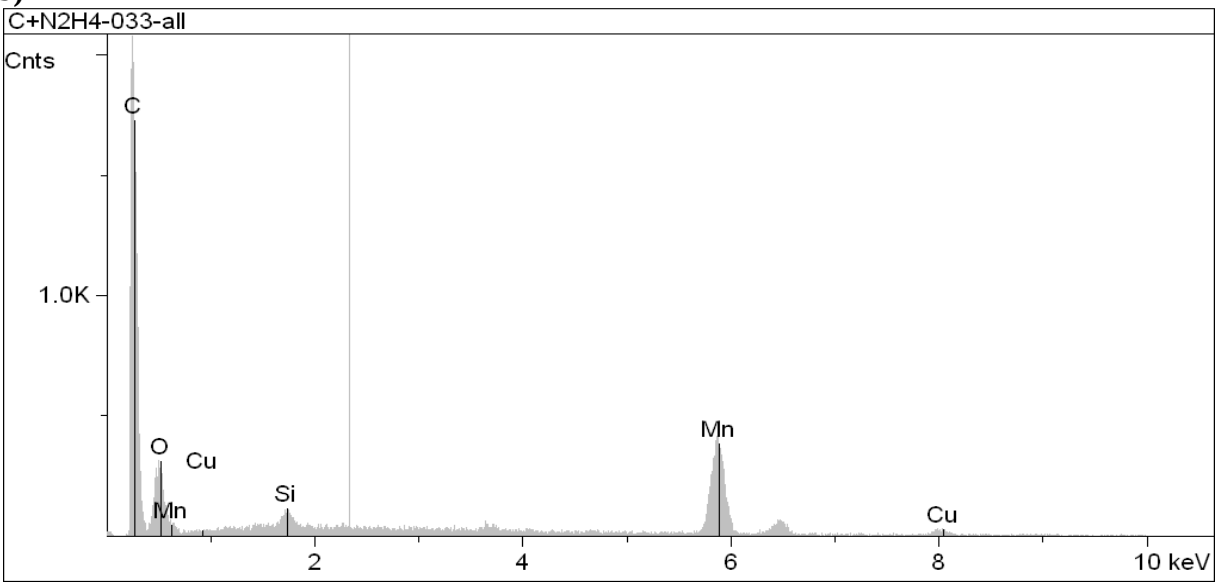

Figure 2.10(a) EDS Spectrum of Graphene Oxide bulk powder showing Oxygen peak at 0.52KeV along with peaks for Manganese and Potassium EDS **(b)** Spectrum of Hydrazine Reduced Graphene nano platelets bulk powder showing reduction in Oxygen peak and residual Manganese peak

The EDS spectrum of Hydrazine Hydrate reduced graphene nanoplatelets, as observed in figure 2.10, confirmed the the removal of oxygen with the reduction in intensity of the peak at 0.52KeV X-ray energy corresponding to oxygen. This was one among other proofs that

Hydrazine hydrate is a valid reducing agent for the reduction of graphene oxide. Also, a significant decrease in the intensity of the manganese peak at 5.90KeV X-ray energy corresponding to that of Manganese shows that, manganese gets removed during the reduction reaction. However, there seemed to exist some level of residual manganese in these material which might be free manganese ions as impurities due to improper dialysis during the synthesis of graphene oxide. In figure 2.11, we observed the peak for Iodine at X-ray energy level 3.94KeV, that are emitted due to the transfer of electrons from the I to L sub-shell in the atomic structure of Iodine. The intensity of the peak although not as significant as that of manganese in the graphene oxide powder, still confirms that there existed a certain amount of Iodine in the sample affirming the ultimate aim of this research thesis.

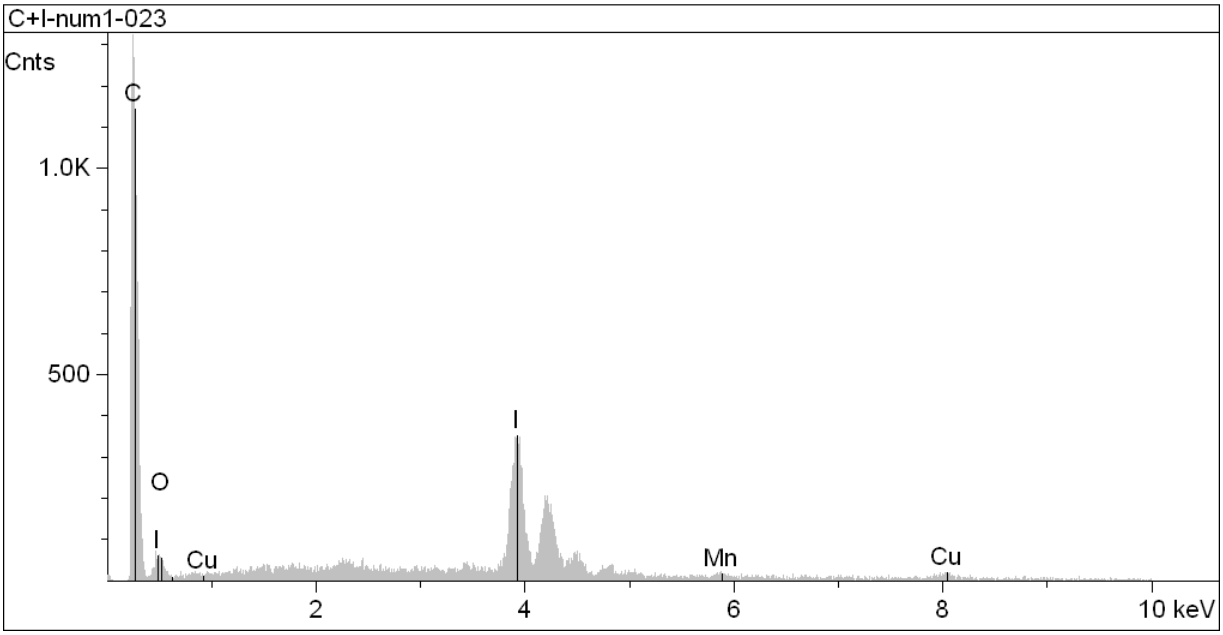

Figure 2.11 EDS Spectrum of Hydrogen Iodide reduced graphene nanoplatelets bulk powder showing Iodine peak 3.94KeV and Oxygen peak of negligible intensity.

Also, the intensity of the oxygen peak is almost absent denoting a possibility that Hydroiodic Acid at 32.1mM concentration is a better reducing agent than Hydrazine Hydrate at 32.1mM concentration.

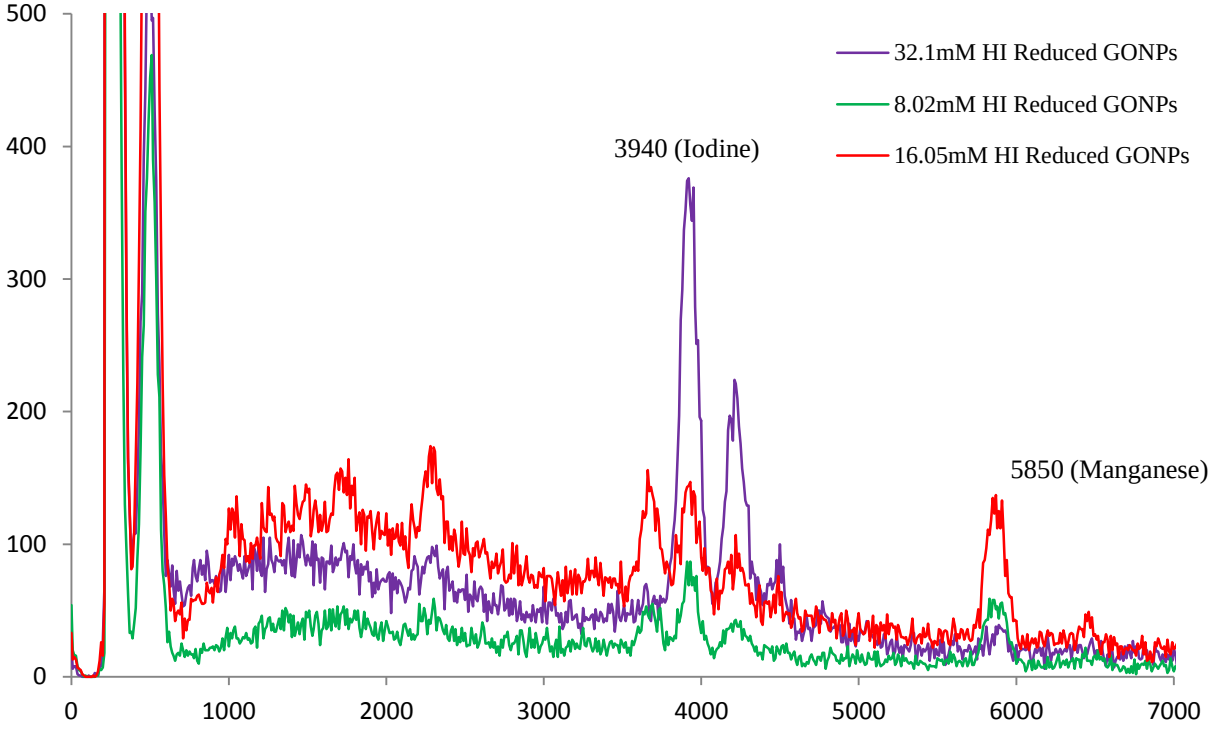

Figure 2.12 Comparison of EDS spectra of Graphene nanoplatelets reduced using different concentrations of Hydrogen Iodide.

It was interesting to observe that the residual managanes in the hydrogen iodide reduced samples was very minimal relative to the residual manganese in the N_2H_4 reduced samples.

EDS spectra for other Hydrogen Iodide reduced samples, using 8.025mM, 16.05mM and 23.45mM concentrations were also obtained. As a comparative study, a graph was plotted with all EDS spectra of all the HI reduced samples to understand how the reduction using the different concentrations of HI worked. In figure 2.12, it was showed that when the 32.1mM concentration of Hydrogen Iodide was used to reduce the graphene oxide, on an average, it contained the highest percentage of Iodine. This lead to an understanding that, there might be possibility that

higher the concentration of Hydrogen Iodide used, higher was the amount of Iodine incorporated. However, this is not a perfectly convinving explanation to prove the above mentioned hypothesis because EDS is a spot based analysis where X-rays are collected only from the specific areas where the electrons beams are shot. They are prone to change with the area from which they are being detected or it might have also be related to the uniformity at which Iodine gets attached to the graphitic structure. Nonetheless, the EDS spectra proved that Iodine can be incorporated in grphene nanoplatelets via HI induced reduction of graphene oxide. Further research was mostly focussed on optimizing the process of iodine incoporation and trying to make these materials close to being used as contrast agents.

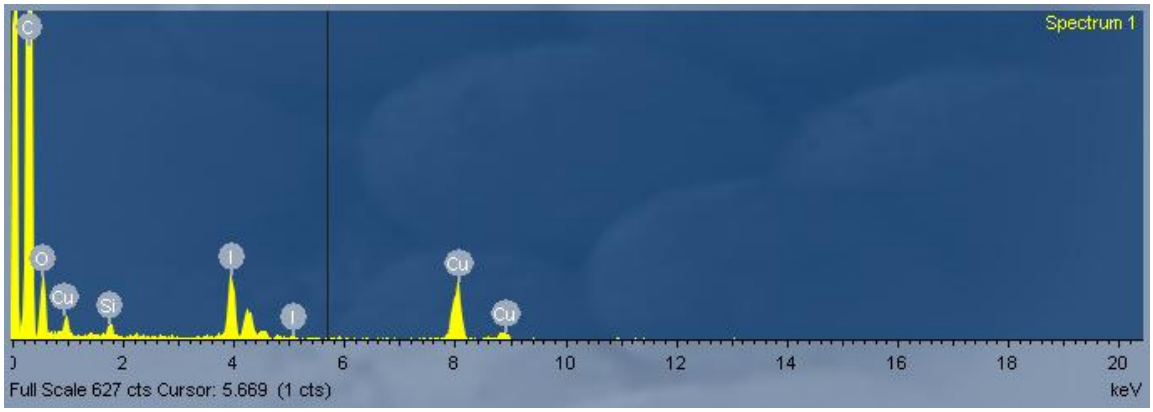

Figure 2.13 HR-TEM/EDS spectrum of 32.1mM HI reduced sample grid A

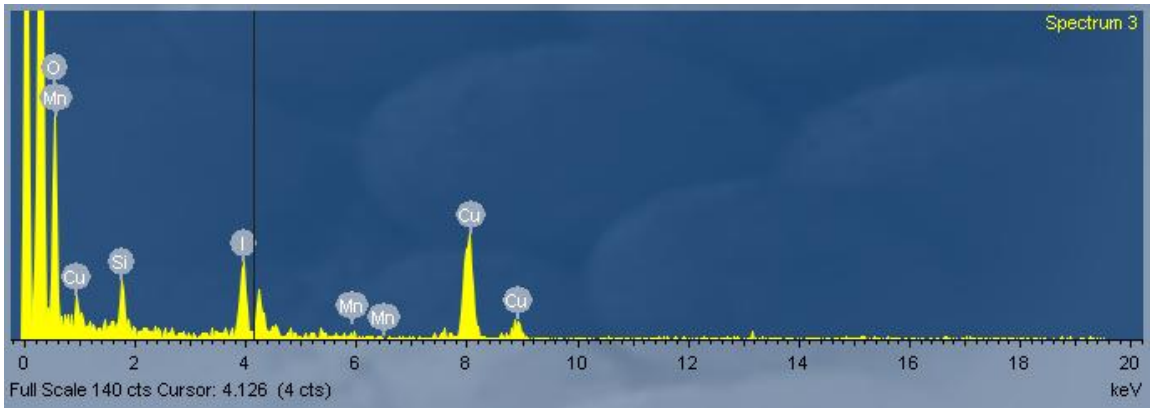

Figure 2.14 HR-TEM/EDS spectrum of 32.1mM HI reduced sample grid B

TEM/EDS was also performed on the 32.1mM HI reduced platelets using the same samples used for obtaining the Low resolution and High resolution TEM images. These spectra also confirmed the presence of Iodine in them, similar to those obtained using the SEM/EDS. It was interesting to note that, the HR-TEM/EDS samples were as low as 1mg/ml solution strained onto grids, which meant that, even at such lower concentration of Iodine loaded graphene nanoplatelets in solution, a distint peak was observed at the 3.94KeV X-ray energy level corresponding to Iodine.

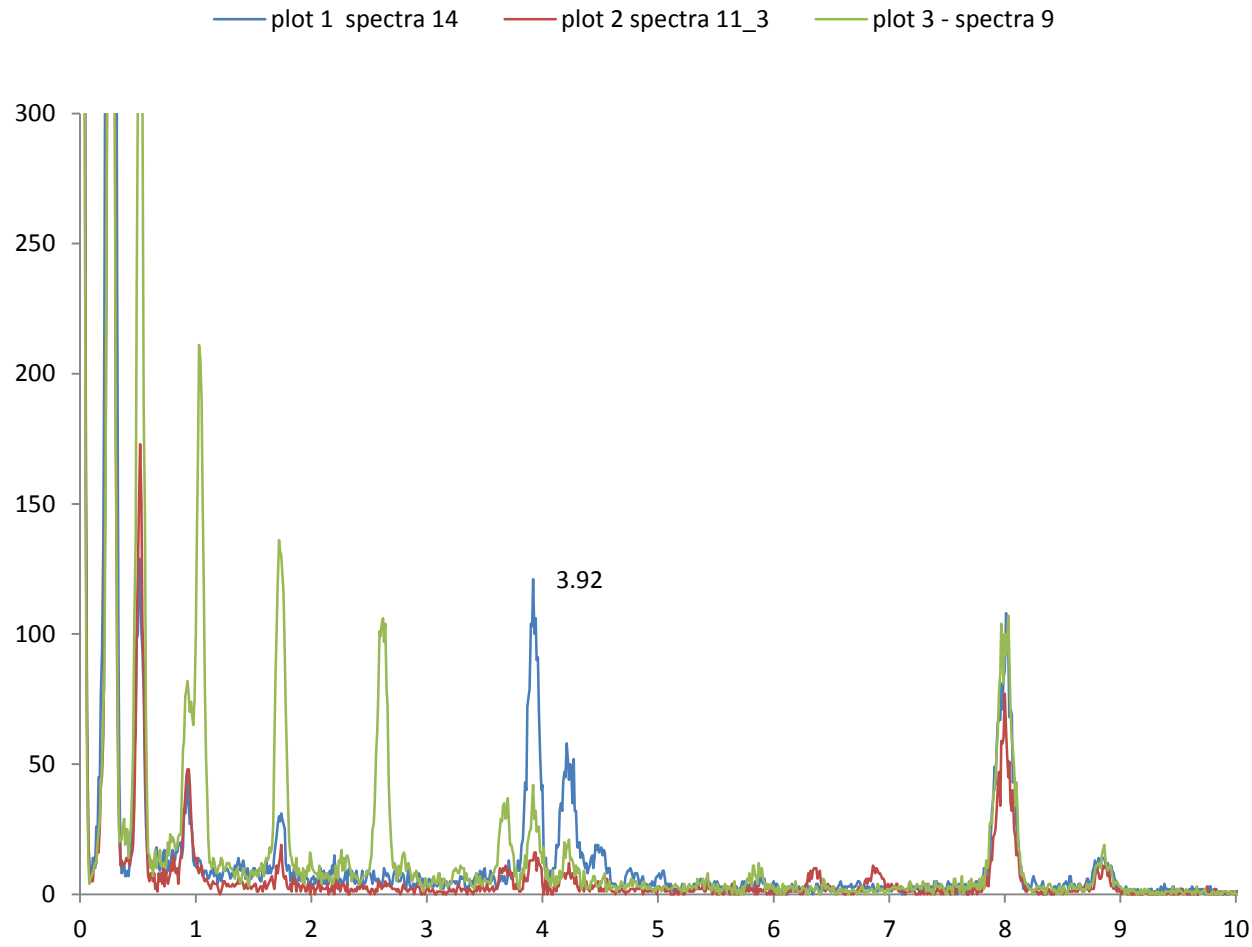

Figure 2.15 Comparison of EDS spectra from HR-TEM/EDS of 32.1mM HI reduced graphene nano platelets

Both the data from the SEM/EDS and HR-TEM/EDS were taken simply as a confirmation for the presence of Iodine and not as a quantitative technique for obtaining the exact amount of Iodine in each different sample. The EDS spectra in Figures 2.13 and 2.14 shows the HR-TEM/EDS spectra of 32.1mM HI reduced samples taken at different locations at ultra high resolution magnification levels. Figure 2.15 shows a illustrative comparison of EDS spectra of the same sample but at different spots of x-ray detection. These spectra were all obtained corresponding to the TEM images and magnifiction parameters simultaneously. X-ray microanalysis proved to be a valuable technique in this research as it directed us in the right direction in our venture to figure out what concentration of Hydroiodic acid used worked best in the Iodination of the graphene material. However, as mentioned earlier, the EDS was not used as a quantitative analytical technique.

II.3.5 X-Ray Diffraction Analysis

X-Ray diffraction technique performed using the Philips Analytical X-ray in the Materials Characterization Laboratory in the Department of Materials Science and Engineering at Stony Brook University. X-Ray Diffraction Technique was mainly used to analyze and investigate the imperfections in the crystalline material structure, atomic arrangement, and also crystallite size. For our research, we decided to use the XRD analysis in order to look for any change in the structure of the material. We know through literature [2], that there is a structural change during the oxidation of Graphite flakes and further change when the bond configuration is restored during the reduction of Graphene Oxide. So, we theorized on tentative grounds to expect prominent differences in the XRD spectra of Graphite, Graphene Oxide and HI reduced Graphene Nano Platelets.

The samples used for XRD analysis needed to be bulk dry powder. The sample holder was a metal slab with a rectangular cavity of dimensions 1.5cm x 1.5cm x 0.05cm. The sample material was to be compressed and compacted in the caivty to that any rotation of the sample holder did not let the material fall out of the cavity. XRD analytical technique followed Bragg's law and the spectra is characteristic of every material. A log book or Card number from the ICDD was used to identify the material for each characteristic peak in the spectrum. Figure 2.16 shows the XRD analysis spectrum of Graphite flakes. It showed a single sharp peak of very high intensity at 26.6º which is characteristic of carbon in its graphitic form. Figure 2.17 shows the XRD analysis of Graphene Oxide powder. In this spectrum the peak at 26.6º was drastically dropped in intensity than that of the graphite peak.

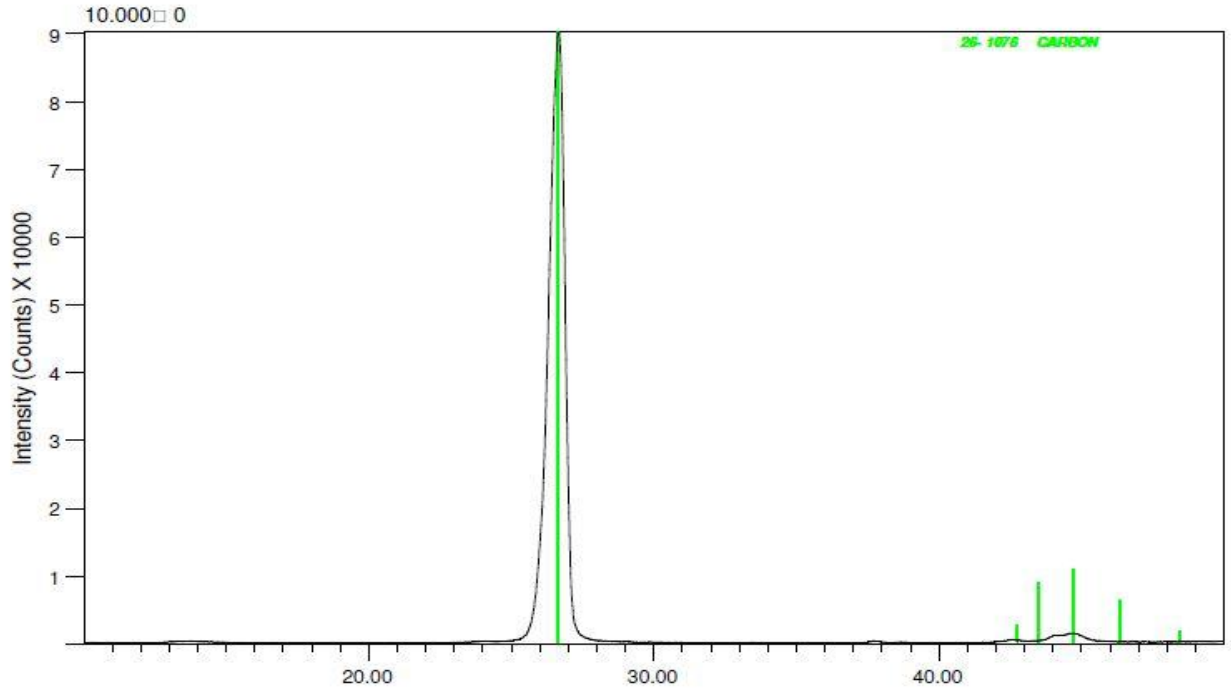

Figure 2.16 XRD spectrum of Graphite Flakes showing a peak at 26.6º

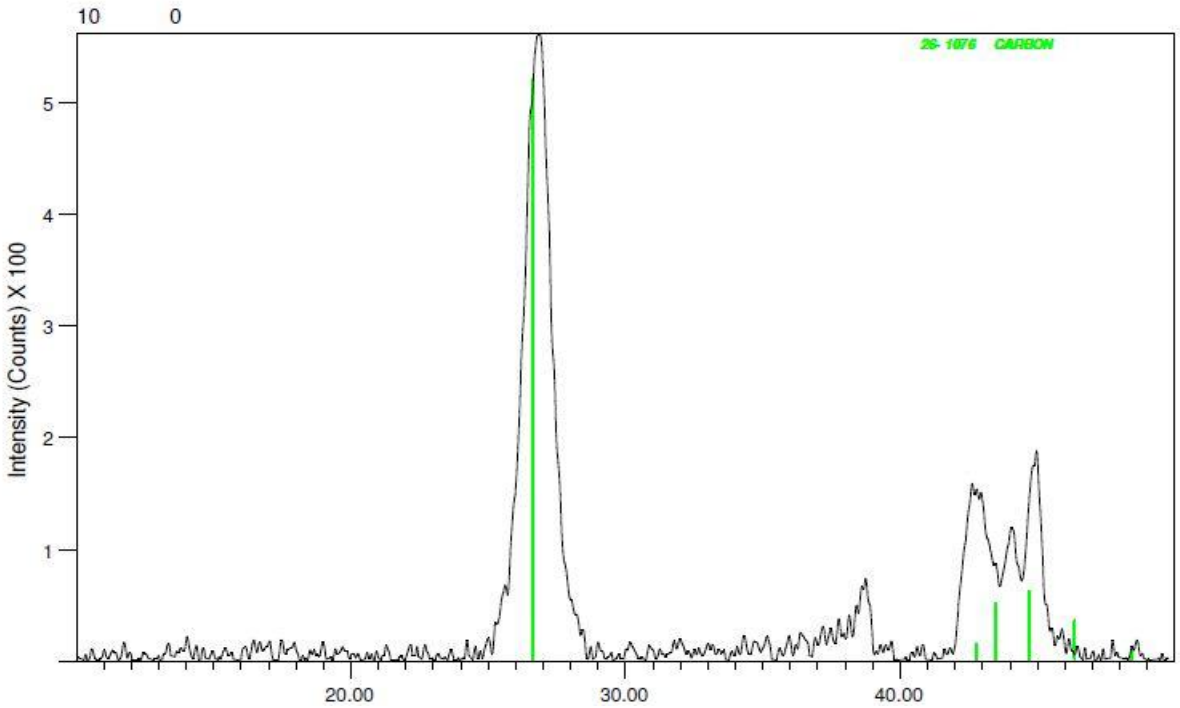

Figure 2.17 XRD spectrum of Graphene Oxide (background subtracted) showing additional peaks at 42.8º and 44.9º and the complete loss of crystalline structure due to oxygenation.

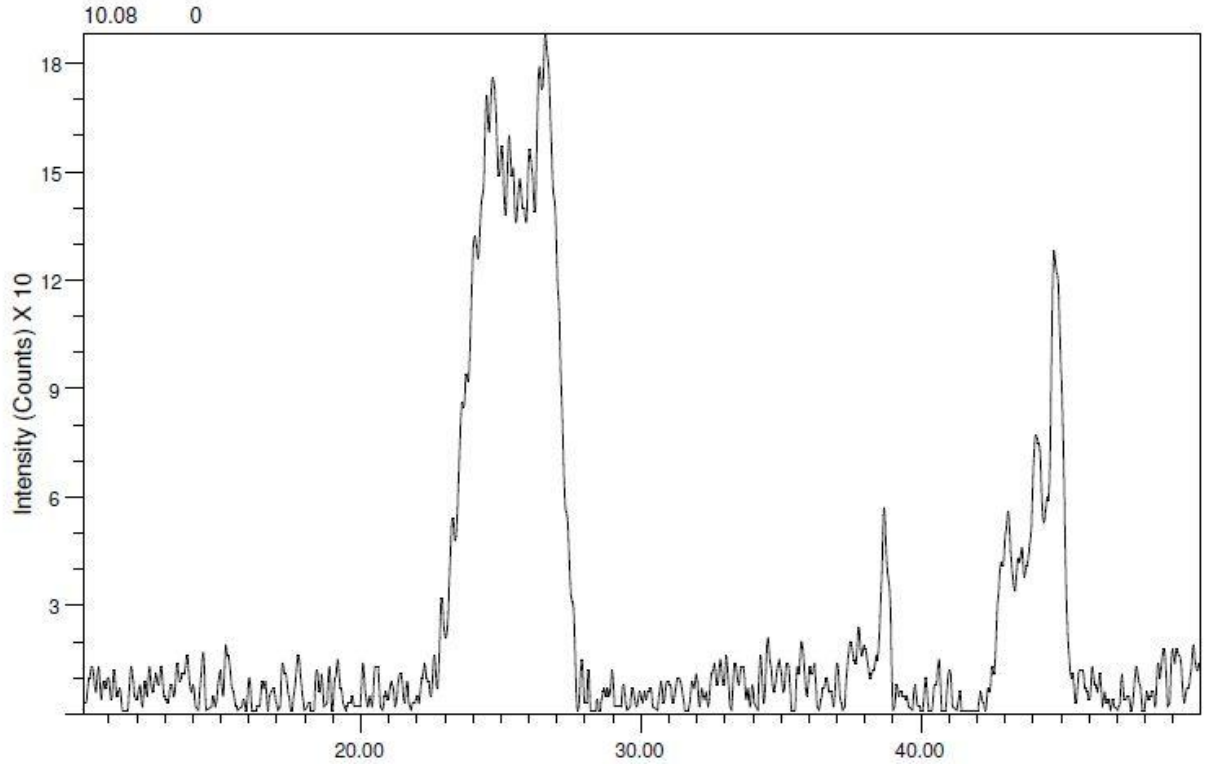

Figure 2.18 XRD spectrum of HI reduced Graphene Nano Platelets showing new peak at 24.4 º

In addition to that, two smaller peaks at 42.8º and 44.9º that were not seen in the Graphite spectrum were also observed. This definitely denotes a change in structure, possibly the change of sp^2 configuration to sp^3 bonding configuration due to the oxidation of Graphite. In figure 2.18, the XRD spectra of HI reduced GNPs showed the same peaks at 26.6º, 42.8º and 44.9º. In addition, a new peak at 24.4º for the HI reduced platelets was observed. The intensity of the peaks of Graphite was the highest and it dropped exponentially through Graphene oxide and reduced graphite. This was because of the step by step loss of cystalline structures in the material. We could also interpret this data to study the possibility that the concentration of HI used was only enough for partial reduction of graphene oxide and not sufficient for a complete reduction. Nonetheless, XRD for our purposes showed difference in the spectra for all three different samples supplementing the theory that Hydroiodic acid reduces graphene oxide.

II.3.6 Raman Spectroscopy

Raman Spectroscopy was performed using the Proraman-L Raman spectrometer and the Enwave Optronics software was used to plot the spectra i.e. the Intensity versus wavenumber curve. Raman Spectra of Graphite and Graphene Oxide, as observed in Figure 2.19 show how clearly the structural changes in the material are reflected in the spectra. The Raman spectrum of pure graphite from flakes showed a sharp peak at wavenumber 1562cm^{-1}. After chemical processing to exfoliate and oxidize the graphite flakes in to graphene oxide, the sp^2 hybridized structures are broken down to form sp^3 with the addition of epoxide and hydroxyl groups. Raman spectra of graphitic structures and some non-graphitic structures generally showed an intense peak around 1582cm^{-1} which was due to the E2g intralayer C-C bond stretching [27]. This intense band was called the ‘G’ band or Graphitic band. In some materials, wherein the actual graphitic

structure was modified or altered, like glass carbon or milled graphite or other materials, a new band arises, of which the G band existed as an overtone. This new band was called the 'D' band or the disordered graphitic band. In our research, the spectroscopic analysis of Graphene oxide showed two peaks. The G band occurred at 1594cm^{-1} with intensity of 232 and the D band at 1358cm^{-1} with an intensity of 167. The intensity ratio of the D band and G band of Graphene Oxide spectrum came to less than unity value of 0.72. Furthermore, the spectrum of Hydroiodic acid reduced graphene nano platelets showed the G band at 1594cm^{-1} and the D band at 1346cm^{-1}. The D/G intensity ratio of the HI reduced graphene nano platelets was about 1.2. This increase in the D/G ratio, from 0.72 for graphene oxide to 1.2 for HI reduced graphene nanosheets signifies a possible restoration of structural properties close to that of pristine graphite. Raman spectra for other graphene nano platelet samples that were reduced using different lower concentrations of Hydroiodic acid were also obtained and analyzed.

In any case, chemical reduction of graphene oxide was confirmed by the increase in the D/G intensity ratio of the reduced samples. The only difference that was observed was the possible variation in the extent of reduction. Evidently, the samples reduced using the highest concentration of Hydroiodic acid showed the most reduction. However, even though the chemical reduction of graphene oxide using HI was confirmed using the Raman spectroscopy, none of this information showed any proof of the presence of Iodine in the HI reduced samples. For this reason, we performed a Micro-Raman combined with scanning probe imaging in order find out any possible evidence to confirm the incorporation of Iodine in the material that was already shown using the Energy Dispersive X-ray spectroscopic technique.

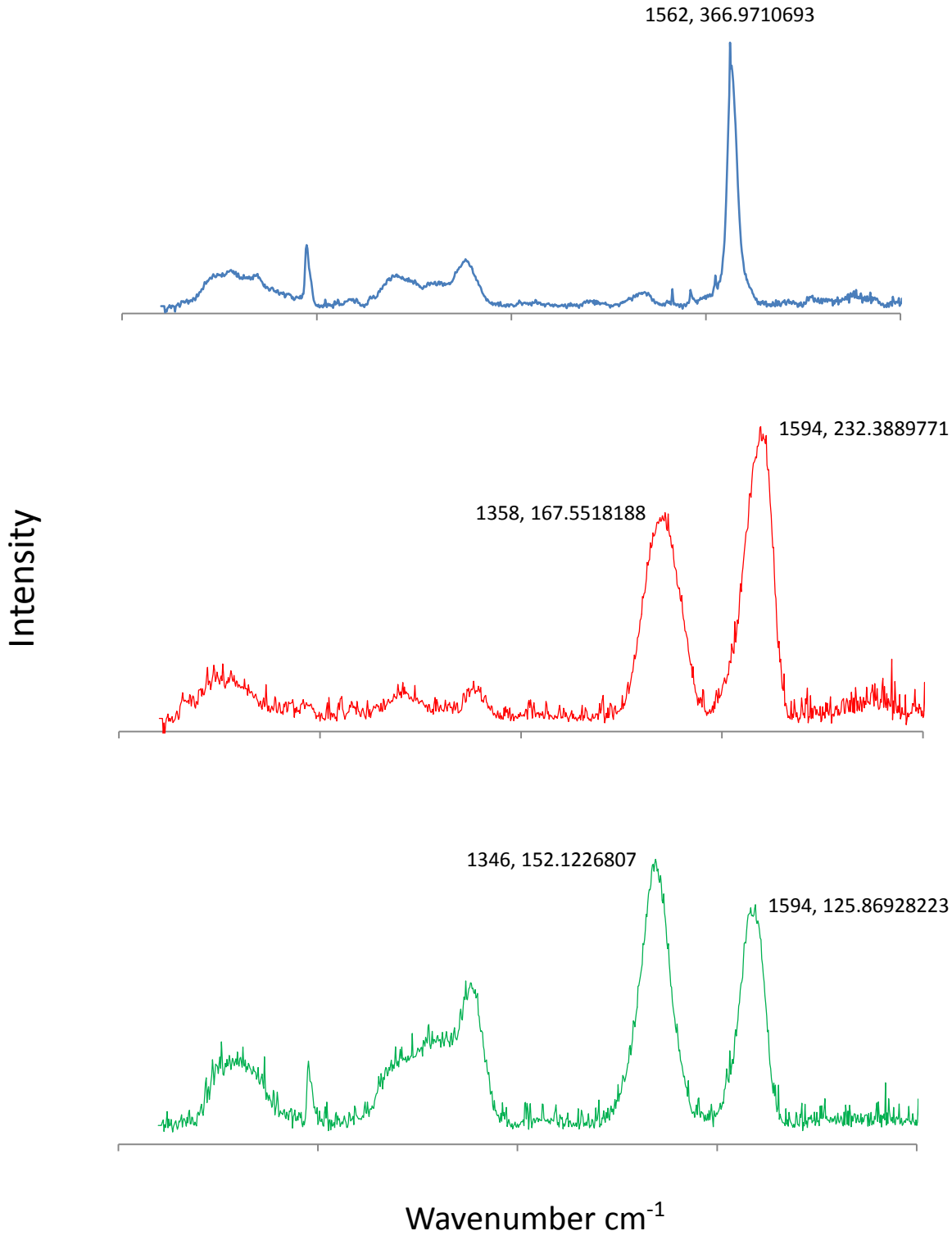

Figure 2.19 Raman Spectra of Graphite (top), Graphene Oxide (middle), 32.1mM HI reduced platelets (bottom)

II.3.7 Micro Raman Imaging

Micro Raman Spectroscopy was performed using the Confocal Raman Micro spectrometer at the Vibrational Spectroscopy Laboratory in the Department of Geosciences, Stony Brook University.

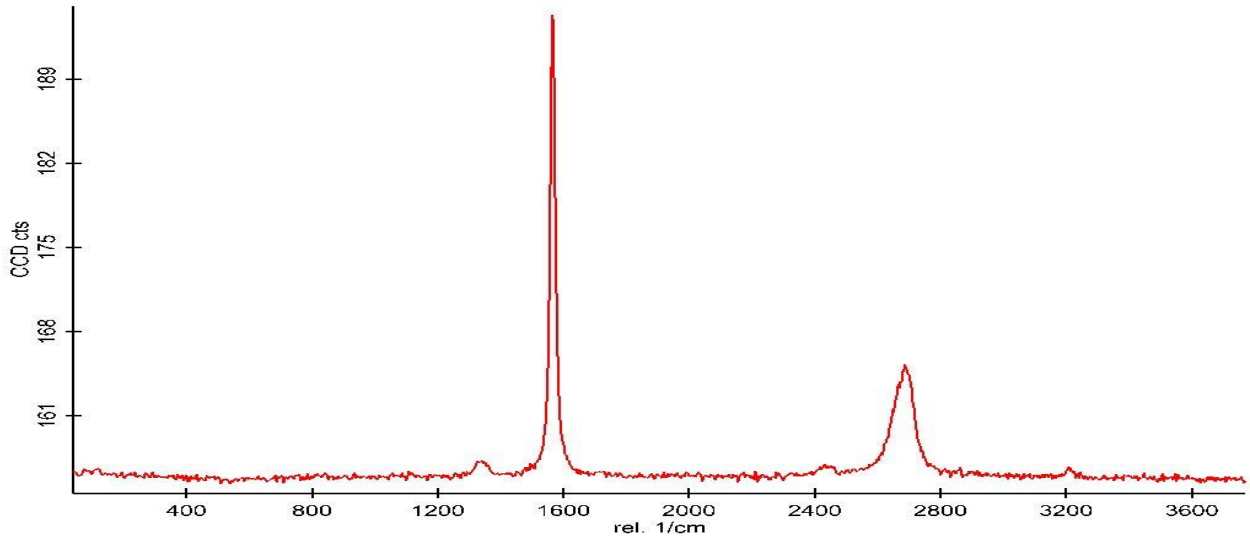

Figure 2.20 Micro Raman Spectra of Graphite

The Micro Raman spectrometer had a very high spatial resolution due to the fact that the excitation laser beam is confined and focused to a diameter at micrometer level. Hence the results obtained using the micro Raman were a lot better than the conventional laboratory Raman setup. We performed a micro Raman spectroscopy on a new batch of graphite, graphene oxide, hydrazine reduced graphene nano platelets and hydrogen iodide reduced graphene nano platelets.

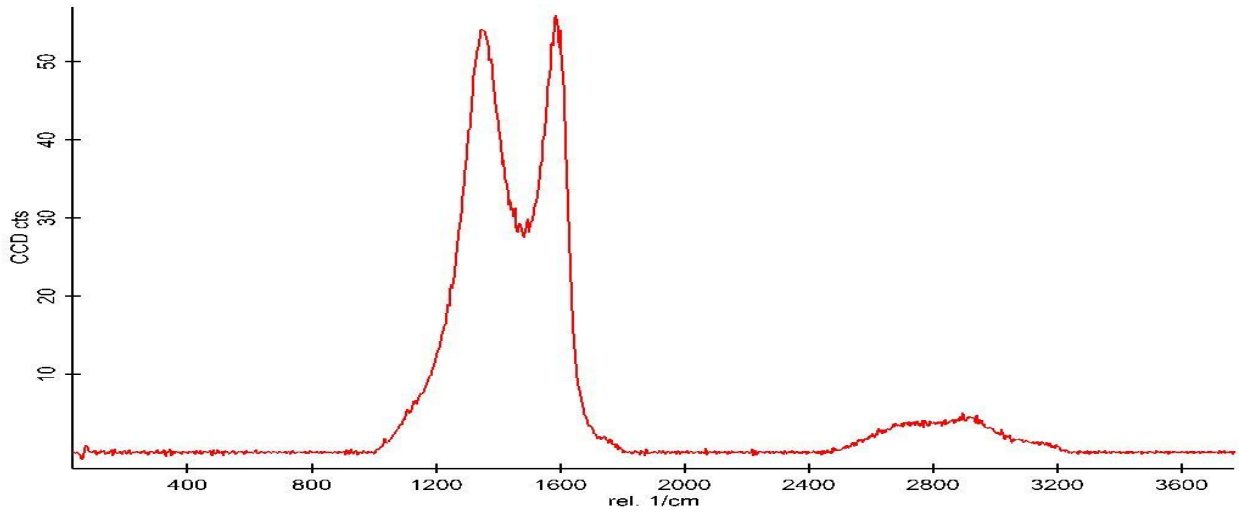

Figure 2.21 Micro Raman spectra of Graphene oxide. D band at 1357cm^{-1} and G band at 1594cm^{-1}

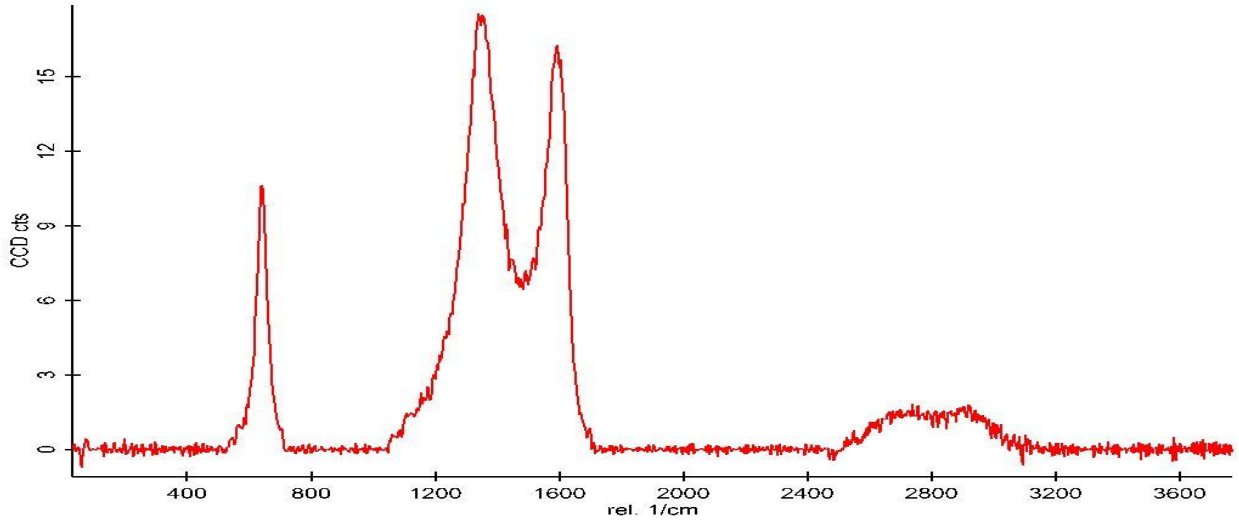

Figure 2.22 Micro Raman spectra of Hydrazine Hydrate graphene nano platelets. D band 1350cm^{-1} and G band 1594cm^{-1}

From figure 2.20 for the micro Raman spectra of pristine graphite, we observed the carbon peak at 1563cm^{-1} at almost the same wavenumber as obtained through the regular Raman setup. After oxidation, the graphene oxide sample yielded the two G and D bands due to the disorder in the graphitic structure. The D band occurred at 1357cm^{-1} and G band at 1594cm^{-1}.

Figure 2.22 with the spectra for Hydrazine Hydrate reduced graphene nano platelets showed mild shift in and D peak at 1350cm^{-1} and G peak at 1594cm^{-1}.

(a)

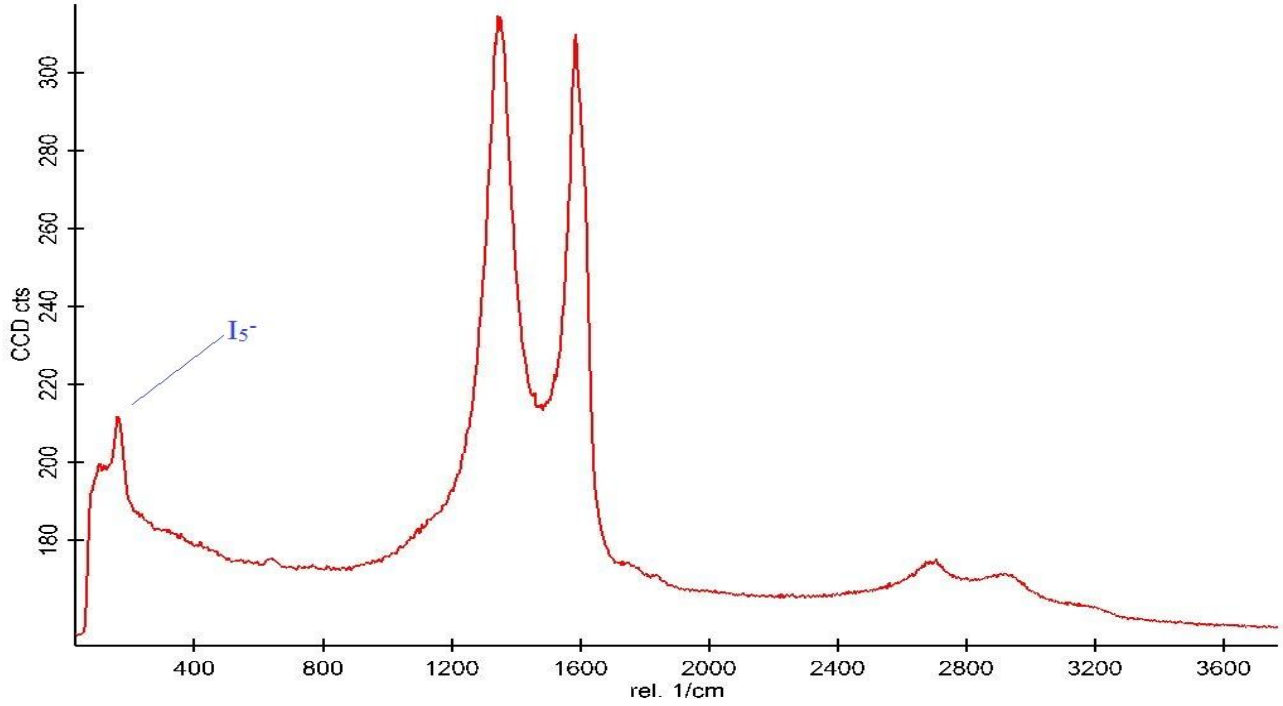

Figure 2.23 (a) Micro Raman spectra of HI reduced platelets showing peak at 154cm^{-1} for pentatiodide.

Similarly, in the Hydroiodic acid reduced samples the D peak was at 1351cm^{-1} and G peak at 1586cm^{-1} (refer Figure 2.23b). An increased D/G intensity ratio was observed for the Hydrazine and Hydrogen Iodide reduced samples than the D/G intensity ratio of Graphene Oxide. Most importantly, the prime reason to have performed the Micro Raman spectroscopy was to observe the tiny peaks between 100cm^{-1} and 200cm^{-1} of the Raman wavenumbers. Interestingly, in Figure 2.23(b) we saw a peak 154cm^{-1}, which was the characteristic peak of Iodine in its pentatiodide state [28].

(b) 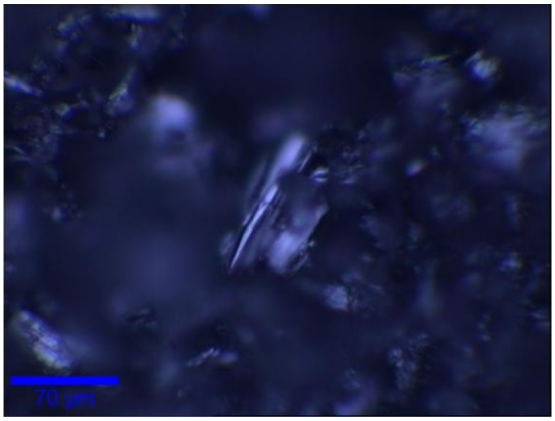

Figure 2.23 (b) Scanning Probe Microscopy Image of HI reduced platelets showing location on sample where the excitation laser was confined and focused

This peak was not seen in the Raman spectra for Hydrazine Reduced samples or Graphene Oxide, which further convinced that the occurrence of this peak was in fact due to the reduction reaction with Hydroiodic acid. However the intensity of the peak was relatively very low with a value of 210 in comparison to the intensity of the D and G peaks that were about 320. Nonetheless, this peak confirmed the presence of Iodine in the sample in its pentatiodide state. A small bump in the spectral plot around 117cm^{-1} is also seen, although not clearly visible denoting the triiodide chemical state. Evidently, the pentatiodide state dominates its presence over the triiodide state. Figure 2.23 (a) is the Scanning Probe Microscopy image of the HI reduced graphene platelets and the area in the center was where exactly the confined laser beam was focused on to the sample.

II.3.8 Ion Selective Electrode Measurements

Ion Selective Electrode measurements were performed on the samples by the scientific staff at Galbraith Laboratories. Prior to the Ion Selective Electrode measurement, the samples were weighed and prepared using Oxygen Flask combustion. Oxidative Combustion or Oxidative Flask Combustion was performed using an Erlenmeyer flask (oxygen flask). Combustion aids were added as necessary and a known volume of absorbing solution was added to the oxygen flask. The flask was purged at atmospheric pressure with oxygen. The flag containing the sample was then ignited and immediately sealed into the flask using a silicone rubber stopper fitted with a solid quart rod. Once combustion was complete, the flask was inverted several times to effect quantitative absorption of the liberated gases. This oxygen flask combustion method was primarily used for the detection of Halogens. The protocols for Oxygen flask combustion and the ion selective electrode measurements were provided by Pat DeLozier of Galbraith Laboratories. These protocols were based on the references from the American Society for Testing and Materials, ASTM E-442, Test Method for Chlorine, Bromine, or Iodine in Organic Compounds by Oxygen Flask Combustion. Also the test methods used by the staff at Galbraith Labs were accredited in accordance with the recognized International Standard ISO/IEC 17025:2005 General Requirements for the Competence of Testing and Calibration Laboratories by the American Association for Laboratory Accreditation.

The following protocol that was followed for the experimental analysis of iodine using Ion-Selective Electrode was provided by the staff at Galbraith Labs. Iodine in its ionic form (I^-) in aqueous solution can be determined potentiometrically using an iodide specific electrode coupled with a pH meter. This test method measured total elemental iodine when used in conjunction with Oxygen flask Combustion. Inorganic iodine was usually measured either

directly or following extraction procedure, or the dissolution procedure. Molecular iodine (I2) and iodate (IO3−) were also measured by this method as they are reduced to (I−) by hydrazine. The concentration of iodide in unknown samples is determined by comparison to a linear regression analysis of known reference standards. The method was very sensitive with a lower limit of quantitation of 0.01 mg/L in solution. The upper range of the method can be extended by dilution. Table 2.1, as provided by Pat DeLozier at Galbraith, shows the brief overview of the equipment used and procedure followed during the analysis.

Instrument	ORION Iodide Electrode (9453); ORION Reference Electrode (90-01 Single-Junction); Fisher Accumet AR25 Ion Meter.	
Preparation	Combust sample in an oxygen rich atmosphere for the determination of total iodine. For the determination of ionic iodide, samples may be read directly or dissolved or leached with ionic strength adjuster solution.	
Calibration	Prepare working standard solutions from the stock I 1000 µg/mL solution in concentrations of 10, 5, 1, 0.1, and 0.05 mg/L.	
Determination	Direct readout in mg/L using an ion meter.	
Precision & Accuracy (p-0902)	RSD of combustion standard, p-53035.7%	RSD of direct standard, p-53054.2%
|Interferences	High concentrations of chloride, bromide, and thiosulfate interfere. Sulfide and cyanides can interfere. Bi, Cd, and Pb can complex the iodide and interfere.	
Calculations	*ppm I = <u>(sample reading – * blank reading) (mL of ISA)</u>* *weight of sample in g* * If sample prep is done by G-54 subtract the blank value from the sample reading. Otherwise do not subtract the blank reading.	

Table 2.1 Protocol for the analysis of Iodine using Ion-Selective Electrode measurement. Provided by Galbraith Laboratories.

Three samples had been sent for analytical testing. All three samples were 32.1mM Hydroiodic acid reduced graphene platelets and each weighed about 100mg. The three samples, namely Batch 1, 2 and 3, were obtained using separate reduction reactions with different mass of starting material (graphene oxide). The yield obtained through each batch was different but it was made sure we had above 100mg in each batch. For the analysis, however, not all the mass was used for oxidative combustion. After the samples were prepared using the above mentioned protocols and tested using the set procedure, the results were finally obtained and received from Galbraith labs through email. Table 2.2 shows the results, as provided (not altered to any decimal value) by Galbraith Labs. We observed that, although there were inconsistencies in the percentage of Iodine in the graphene nano platelets, a range of 9%-12% Iodine was definitely present in the material.

Sample	Amount of sample tested	Percentage of Iodine present
32.1mM HI reduced GNPs Batch 1	37.40 mg	9.89%
32.1mM HI reduced GNPs Batch 2	31.07mg	11.78%
32.1mM HI reduced GNPs Batch 3	31.89mg	9.97%

Table 2.2 Test results of Ion Selective Electrode measurements on different batches of 32.1mM HI reduced Graphene Nano Platelets showing percentage of Iodine in each sample.

So far, all the testing and analytical techniques that have been used to characterize the material have concentrated only the morphology, structure, Chemical reduction and Elemental Analysis. Having proved that Iodine exists in the samples as pentaiodides, the next major

experiment was to run experiments to find out if these Iodine laden graphene nano platelets could be prospective candidates for the fabrication of a CT contrast media.

II.3.9 CT Phantoms

CT Phantoms or simply Phantoms are objects, mostly made of water or water equivalent plastic. The CT number of water is 0 and hence can be used as a control. The important purpose of using a phantom in CT imaging is to calibrate and fine tune the imaging capabilities of the equipment. At the same, using an object to fine tune the imaging ability avoids the risk of having an actual living subject. The design of phantoms would be based on their use, depending on whether they would be used for 2D or 3D imaging techniques. For our experimental purposes, we used the CT Phantoms at the Stony Brook University Medical Center.

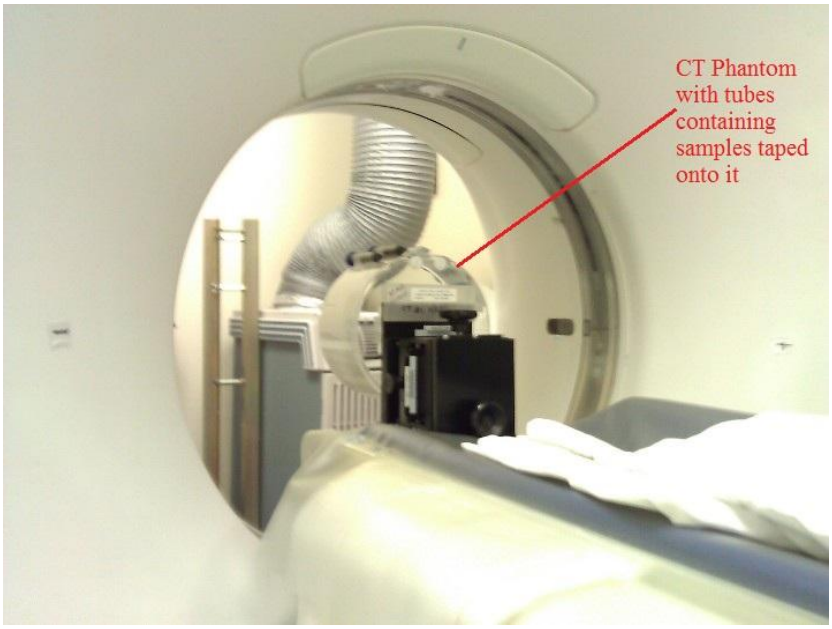

Figure 2.24 Photograph of CT Phantom with falcon tubes containing sample material taped onto it; moving back and forth through the CT scanner.

Four different tubes each containing different material was used for the CT phantoms. Tube 1 contained DI water, tube 2 contained diluted Hydroiodic Acid, tube 3 contained

Manganese Chloride and tube 4 contained iodine laden graphene nanoplatelets. Initially for a test run on the sample, a 1mg/ml solution concentration was prepared. The tubes were well sonicated to disperse the particles thoroughly in water. They were then taped horizontally onto the phantom. The scanner was started and the phantom moved back and forth through it as the scanner took image slices at different positions. The images were obtained on a computer screen for study. However, the first run using the 1mg/ml concentration solution did not show any difference in the contrast on the computer screen. The contrast was zero and similar to that of the DI water and the water inside the phantom.

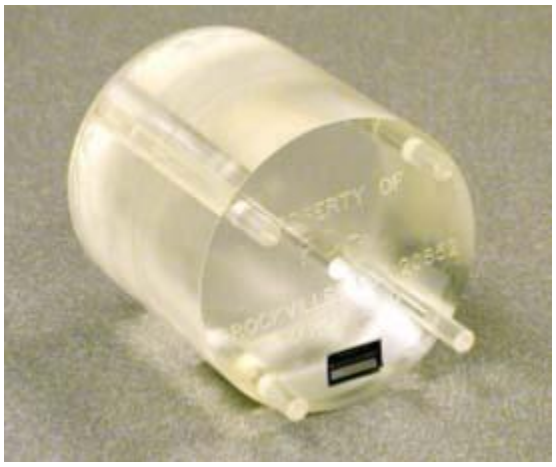

Figure 2.25 CT Head Phantom; Reprinted from Radiation-Emitting Products, *U.S Department of Health and Human Services, FDA*. (Not the actual phantom used for our analysis, but a similar one)

After running the first CT phantom experiment, it was understood that at such low concentrations there was not enough iodine in the samples to give contrast during the scan. So, based on the Ion-Selective Electrode measurements that showed 10% iodine in the 32.1mM GNPs, we prepared a solution with approximately 4mg-5mg per ml iodine concentration. This mixture was transferred to tube 4 and taped onto the phantom along with the three tubes in the

order as mentioned earlier in this section. The scanner was started and head phantoms were taken at 80kV and 120kV obtaining image slices are three different locations on the tubes.

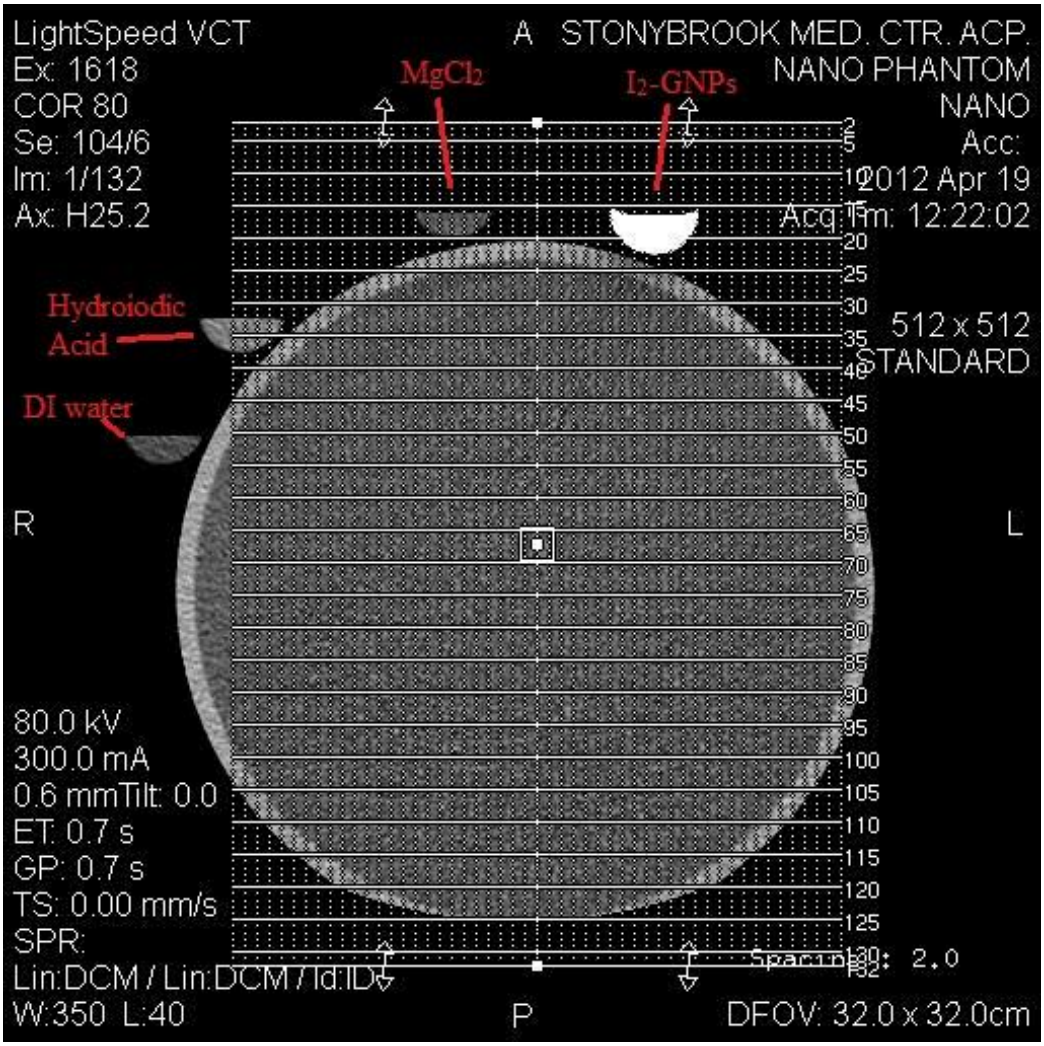

Figure 2.26 CT Phantom image at 80kV showing distinct contrast of HI reduced GNPs (crescent shape at top right) relative to poor contrast of deionized water (extreme left), HI control solution (second from left) and $MgCl_2$ (Manganese Chloride) solution (third from left).

In the above image in figure 2.26 obtained from the CT scanner at 80kV voltage and 300 mA current, we observed a distinct contrast density for the Iodine loaded GNPs with reference to the HI acid solution, Manganese Chloride and water. Figure 2.27 shows the CT

image taken from a different slice but at the same 80kV voltage. Here, we observe that the contrast density of Iodine loaded graphene nano platelets at 4mg/ml concentration is still higher than that of the Hydroiodic acid solution.

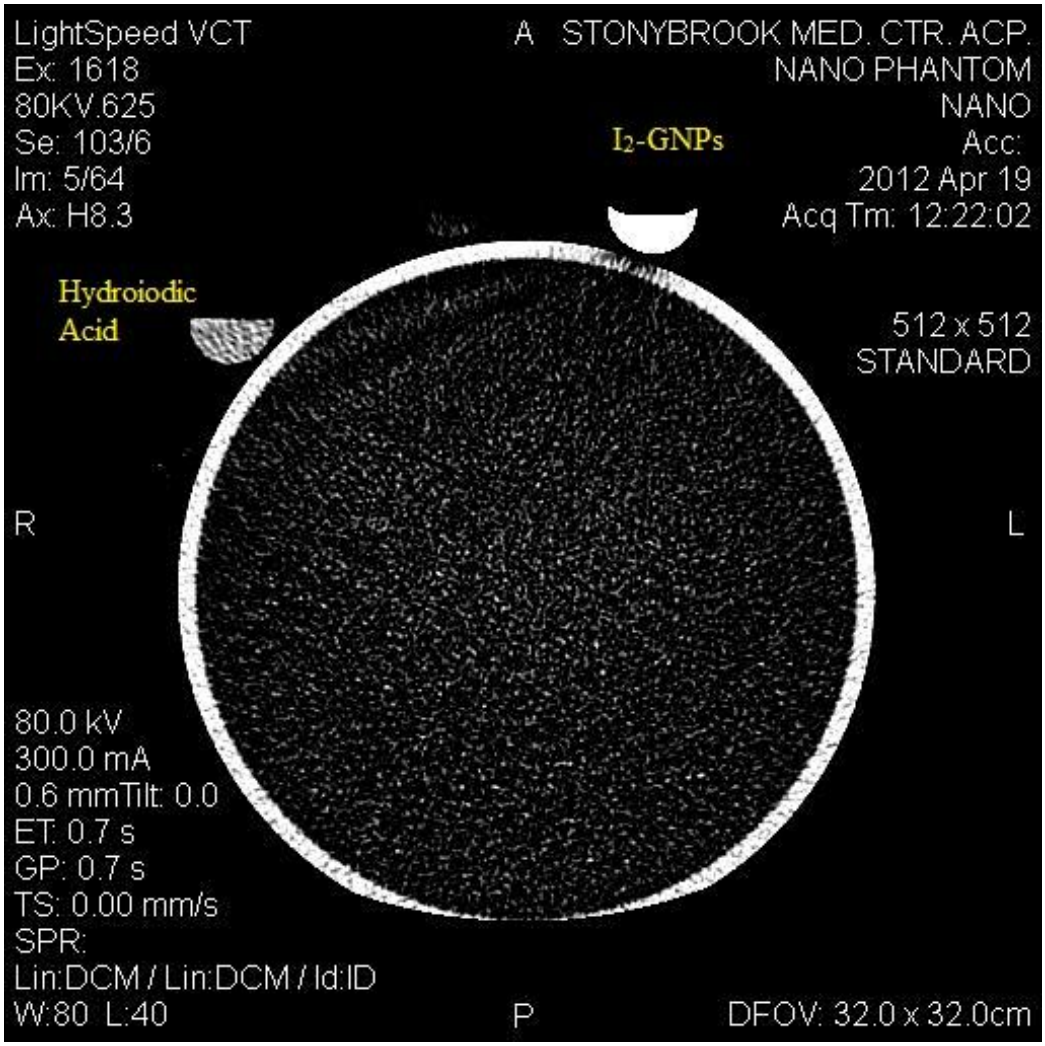

Figure 2.27 CT Phantom image at 80kV showing CT contrast of HI reduced GNPs (crescent shape at top right) than HI control solution (visible extreme left). Contrast of deionized water and $MgCl_2$ (Manganese Chloride) solution are not visible.

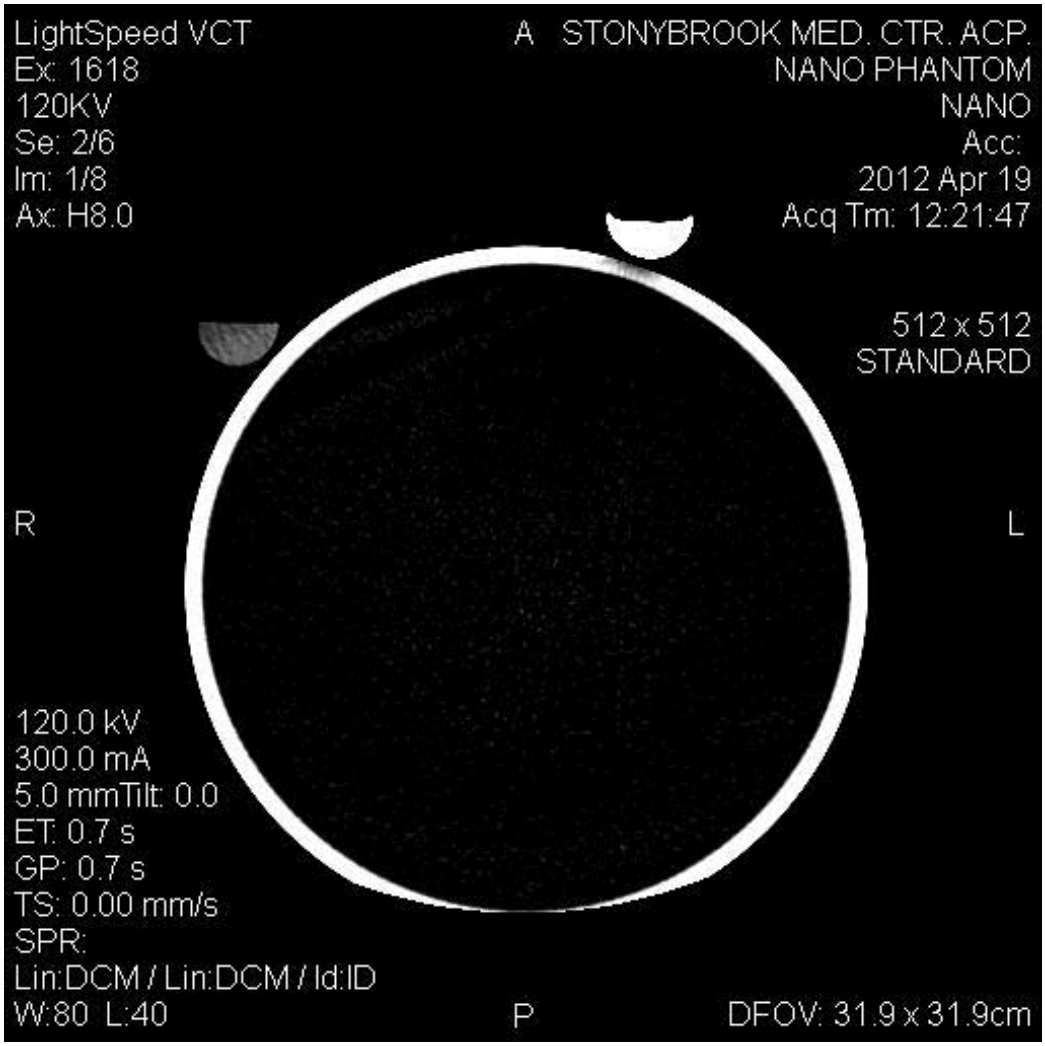

Figure 2.28 CT Phantom image at 120kV showing better CT contrast of HI reduced GNPs (crescent shape at top right) than HI control solution.

However, the contrast density of DI water and $MgCl_2$ were almost negligible as their images were totally blacked out. In figure 2.28, the CT image was from another slice on the phantom and at a higher voltage of 120kV. Again, here the contrast density of Iodine loaded GNPs is relatively better than the control Hydroiodic acid solution. One could clearly see a difference in the contrast density of the samples between the 80kV and 120kV.

Chapter III

Potential Contrast Agents

III.1 Iodinated Graphene nanoplatelets as potential contrast agents

In this research thesis, we have attempted a new route in fabricating X-ray contrast media and have taken a first step in the conceptually right direction by proposing Iodine loaded Graphene nanoplatelets as one of the future materials for Medical Imaging applications. The interesting part of this research was to try and prove that there were ways for Iodine incorporation into the graphitic structure of Graphene Nano Platelets. In our research, we used the reduction route of graphene oxide to Graphene sheets as the method of incorporating Iodine. This not only would interest researchers and scientists to look further into this subject but also will eventually lead to the discovery of other fascinating ways Iodine or any other radiopaque material to be attached to graphene for medical imaging purposes.

The experimental results from this research show that Iodine, in the form of triiodide and pentatiodide exists in different ratios by attaching itself to various locations in the structure of Graphene. Further investigation in this area on how exactly the mechanism of reduction of graphene oxide using Hydroiodic Acid takes place is yet to be brought to limelight. Even though there are a few proposed routes of reduction mechanisms for the reduction of GO using Hydrazine, it has not yet been proved to be the exact mechanism. Ample investigatory work on these subjects of Hydrogen Iodide and Hydrazine Hydrate reduction will eventually allow us to understand the mechanism which in turn will open gateways to the understanding of how Iodine is getting bonded to the Graphitic structure. With this knowledge, the amount of Iodine that can be chemically incorporated into the Graphene can be controlled with the various parameters such as the concentration of reagents, length of reaction, temperature and so on. As stated in literature, the amount of Iodine in the commercially available contrast agents is 150mg/ml or higher. Keeping in mind, the maximum permissible Iodine concentration that would not pose any health

hazard or toxicity to the persons administered with the CA, the Iodine concentration can be carefully constructed into the base material.

III.2 Water soluble Graphene nano platelets

One of the important things that should be given importance while developing a contrast agent of any kind, MRI or CT, is the water solubility of the material that is being used as the contrast media. Graphene oxide by itself is highly hydrophilic and readily allows water intercalation in its layered structure due to the presence of high ratio of oxygenated groups. However, when reduced using Hydrazine Hydrate or Hydroiodic Acid the oxygen groups in GO are stripped off and the sp^2 bond configurations are partially or completely restored. This reduction was mainly carried out in order to make the Graphene electrically conductive similar to that of Graphite. However, since we have used this reduction route, in this research, to reduce the GO and simultaneously incorporate Iodine in them, the water solubility of the reduced graphene oxide powder is poor compared to that of graphene oxide particles. In an attempt to make these particles water soluble, we proposed to coat the graphene nano platelets with a biocompatible surface coating material, such as Dextran.

III.2.1 Dextran

Dextran is a complex very high molecular weight polysaccharide made of many molecules of glucose. The properties and characteristics of Dextran make it highly usable and essential in the fields of biomaterials, pharmacology, agriculture and medicine. Dextran, apart from having the ability to remain stable for up to 5 years are attractive to biomedical researches due to its structural stability, ability to be easily processed, biodegradability, water solubility and biocompatibility.

Dextran has been extensively used in the early and recent past for various biomaterial coatings that include, but are not limited to, iron oxide, quantum dots, graphene oxide, carbon nanotubes and so on [28,29]. We attempted to use Dextran in the course of our research to chemically coat the Iodine loaded graphene nano platelets in order to render possible water solubility to the material, which if worked would pass one of the most essential characteristics of a medical contrast agent.

Dextran T_{10} was added to Hydrogen Iodide reduced graphene oxide in the ratio of 1:10. DI water was used to disperse the powder in a 1:1 ratio. After ultrasonication for 45 minutes to 1 hour in a round bottomed flask, the mixture was heated in an oil bath at 95 degree Celsius under a water cooled condenser that circulated water from an ice cold water bath. The reaction was allowed to proceed for 4 hours before being cooled and centrifuged. However, unlike the other post-reaction centrifugation, in that case the supernatant was not discarded but collected and stored for lyophilization. The supernatant was later placed in the lyophilizer for 48 hours before obtaining the final product.

III.2.2 Iodine loaded Dextran coated Graphene nano platelets

Our experiment, based on previously published literature on Dextran coating and its applications in biomedicine, on dextran coating of Hydrogen Iodine reduced graphene nano platelets although not completely infirm, was still a trial run to make water soluble graphene nanosheets. The lyophilization of the HI-Reduced-Dextran coated GNP supernatant did not yield the amount of material that would be sufficient for any type of characterization and analysis. So, we performed the CT phantom scout run on the non-lyophilized supernatant. The 32.1mM HI reduced-dex samples and 16.05mM HI reduced-dex samples were used and it was interesting to

observe that even though the 32.1mM HI reduced non-dex platelets contained significantly more Iodine than the 16.05mM HI reduced non-dex platelets, the results seemed to be reversed when they were coated with Dextran.

Figure 3.1 32.1mM HI reduced and Dextran coated I_2-GNPs (left), 16.05mM HI reduced and Dextran coated I_2-GNPs (right)

One of the possible explanations for this result could be that the amount of Iodine that was in solution after Dextran coating of the HI reduced platelets was higher when a lower concentration of HI was used for the reduction. The 32.1mM HI reduced GNPs were soluble in water to some extent; whereas the 16.05mM HI reduced GNPs were relatively more soluble. Figure 3.1 shows the deep black color of the 16.05mM HI reduced GNPs vial with respect to the 32.1mM solution. However, this was just a conjecture in the research. There was no clear evidence to quantify which samples had higher amount of Iodine associated within their structure in whichever possible chemical state after the Dextran coating. Further literary and experimental investigations on this specific subject would lead to a substantial conclusion. Also, other parameters influencing these results would be process of Dextran coating the platelets. Ongoing research would also focus on optimizing this process in order to verify if the dextran truly renders complete or partial water solubility when coated on graphene.

III.3 Possible alternatives for X-Ray contrast agents using Graphene

In Kissell and Wilson's thesis research paper, they had explored the possibility of using single walled carbon nanotube filled with Iodine for computed tomographic imaging applications. Their first attempt at the hypothesis of using SWCNTs filled with iodine was successful at the laboratory research level and the idea of development of other possible iodinated contrast agents using graphitic materials were germinated. We have also performed literary surveys and found out that there could be more than fewer ways to incorporate Iodine or Barium or other radiopaque materials in graphitic structures. They could be minor alterations and optimizations in the synthesis, including other intermediate reactions, other ways of restoring sp^2 bonds in graphene oxide and so on. Nonetheless, incorporating these radiocontrast materials would be the most challenging part of any research in this area.

III.4 Conclusions and Future directions

The sole purpose of this research was to prove that Iodine, one of the predominantly used radio contrast material, can be incorporated into Graphitic structures for prospective use as a CT contrast agent. Here, we have shown the reduction route for Iodine incorporation in GNPs. The same concept can also be applied to Graphene nano ribbons and analyze their characteristics and behavior. This paper does not discuss about the bio compatibility and other essential issues in fabricating a contrast agent. However, further research will be focused on subjects such as biocompatibility, cytotoxicity tests, cellular targeting and so on in pursuit of making this material a convincing candidate for contrast agents. Another fascinating part of this project was the presence of residual Manganese along with Iodine in the Hydroiodic acid reduced GNPs. This gives way to a whole new chapter where the manganese present could be optimized and the

material possibly developed into an MRO contrast agent. Such a material has never been developed before and that only adds to the measure of innovative ideas that would create a breakthrough in the near of far future. This thesis presents a series of preliminary ideas that would lead to the continued development and research in the field of CT contrast agents.

References:

1. William S. Hummers Jr., Richard E. Offeman "Preparation of Graphitic Oxide" *Journal of the American Chemical Society* 1958 *80* (6), 1339-1339
2. Stankovich, S., D. A. Dikin, et al. (2007). "Synthesis of Graphene-based nanosheets via chemical reduction of exfoliated graphite oxide." *Carbon 45(7): 1558-1565*.
3. Shin, H.-J., K. K. Kim, et al. (2009). "Efficient Reduction of Graphite Oxide by Sodium Borohydride and Its Effect on Electrical Conductance." *Advanced Functional Materials 19(12): 1987-1992.*
4. Kroto, H. W., J. R. Heath, et al. (1985). "C60: Buckminsterfullerene." *Nature* 318(6042): 162-163.
5. Iijima, S. (1991). "Helical microtubules of graphitic carbon." *Nature* 354(6348): 56-58.
6. Novoselov, K. S., A. K. Geim, et al. (2004). "Electric Field Effect in Atomically Thin Carbon Films." *Science* 306(5696): 666-669.
7. Boukhvalov, D. W. and M. I. Katsnelson (2009). "Chemical functionalization of graphene." *Journal of Physics: Condensed Matter* 21(34): 344205.
8. Iijima S. "Helical microtubules of graphitic carbon". *Nature*. 1991;354(6348):56–8
9. Markovic ZM, Harhaji-Trajkovic LM, Todorovic-Markovic BM et al. "In vitro comparison of the photothermal anticancer activity of graphene nanoparticles and carbon nanotubes". *Biomaterials* 32, 1121–1129 (2010)
10. Dreyer, D. R., S. Park, et al. (2010). "The chemistry of graphene oxide." *Chemical Society Reviews* 39(1): 228-240.
11. He H, Riedl T, Lerf A, Klinowski J. "Solid-state NMR studies of the structure of graphite oxide". *J Phys Chem* 1996; 100(51):19954–8.
12. He H, Klinowski J, Forster M, Lerf A. "A new structural model for graphite oxide". *Chem Phys Lett* 1998; 287(1,2):53–6.
13. Mkhoyan, K., A. Contryman, et al. (2010). "Atomic and Electronic Structure of Graphene-Oxide." *Microscopy and Microanalysis* 16(SupplementS2): 1704-1705.
14. Chen, W., L. Yan, et al. (2010). "Chemical Reduction of Graphene Oxide to Graphene by Sulfur-Containing Compounds." *The Journal of Physical Chemistry* C 114(47): 19885-19890.
15. Zhou, X., J. Zhang, et al. (2011). "Reducing Graphene Oxide via Hydroxylamine: A Simple and Efficient Route to Graphene." *The Journal of Physical Chemistry* C 115(24): 11957-11961.
16. Wakeland, S., R. Martinez, et al. (2010). "Production of graphene from graphite oxide using urea as expansion–reduction agent." *Carbon* 48(12): 3463-3470.
17. Hofmann, U. & Frenzel, A. The reduction of graphite oxide with hydrogen sulphide. Kolloid-Zeitschrift 68, 149–151 (1934).
18. Park, S. & Ruoff, R. S. Chemical methods for the production of graphenes. *Nature Nanotech*. 4, 217–224 (2009).
19. Muszynski, R., Seger, B. & Kamat, P. V. Decorating graphene sheets with gold nanoparticles. *J. Phys. Chem*. C 112, 5263–5266 (2008).
20. Stankovich, S. et al. Graphene-based composite materials. *Nature* 442, 282–286 (2006).
21. Wang, G. X. et al. Facile synthesis and characterization of graphene nanosheets. *J. Phys. Chem. C* 112, 8192–8195 (2008).
22. Gao, W., Alemany, L. B., Ci, L. & Ajayan, P. M. New insights into the structure and reduction of graphite oxide. *Nature Chem*. 1, 403–408 (2009).

23. Fan, Z. et al. An environmentally friendly and efficient route for the reduction of graphene oxide by aluminum powder. *Carbon* 48, 1686–1689 (2010).
24. Skinner, H. F. (1990). "Methamphetamine synthesis via hydriodic acid/red phosphorus reduction of ephedrine." *Forensic Science International* 48(2): 123-134.
25. Stankovich, S., R. D. Piner, et al. (2006). "Stable aqueous dispersions of graphitic nanoplatelets via the reduction of exfoliated graphite oxide in the presence of poly (sodium 4-styrenesulfonate)." *Journal of Materials Chemistry* 16(2): 155-158
26. Geng, Y., S. J. Wang, et al. (2009). "Preparation of graphite nanoplatelets and graphene sheets." *Journal of Colloid and Interface Science* 336(2): 592-598.
27. Yao, Z., H. Nie, et al. (2012). "Catalyst-free synthesis of iodine-doped graphene via a facile thermal annealing process and its use for electrocatalytic oxygen reduction in an alkaline medium." *Chemical Communications* 48(7): 1027-1029.
28. Kyle Ryan Kissell, W. Lon J "Preparation of iodine SWNTs and iodine US-tubes: Synthesis and spectroscopic characterization of iodine-loaded SWNTs for computed-tomography molecular imaging." Rice University Dissertation. 86: 1-10.
29. Goodwin, A. P., S. M. Tabakman, et al. (2008). "Phospholipid−Dextran with a Single Coupling Point: A Useful Amphiphile for Functionalization of Nanomaterials." Journal of the American Chemical Society 131(1): 289-296.
30. Thomsen, H. S. and S. K. Morcos (2000). "Radiographic contrast media." BJU International.
31. Torsten Almén and Peter Aspelin, Medcyclopedia™ Standard Edition, General Electric Healthcare.
32. Standard Reference Data (SRD), The National Institute of Standards and Technology (NIST).
33. Rangel, N. L., J. C. Sotelo, et al. (2009). "Mechanism of carbon nanotubes unzipping into graphene ribbons." The Journal of Chemical Physics 131(3): 031105.
34. Cano-Marquez, A. G., F. J. Rodriguez-Macias, et al. (2009). "Ex-MWNTs: graphene sheets and ribbons produced by lithium intercalation and exfoliation of carbon nanotubes." Nano Lett 9(4): 1527-1533.
35. Cataldo, F., O. Ursini, et al. (2011). "Graphite Oxide and Graphene Nanoribbons Reduction with Hydrogen Iodide." Fullerenes, Nanotubes and Carbon Nanostructures 19(5): 461-468.

APPENDIX

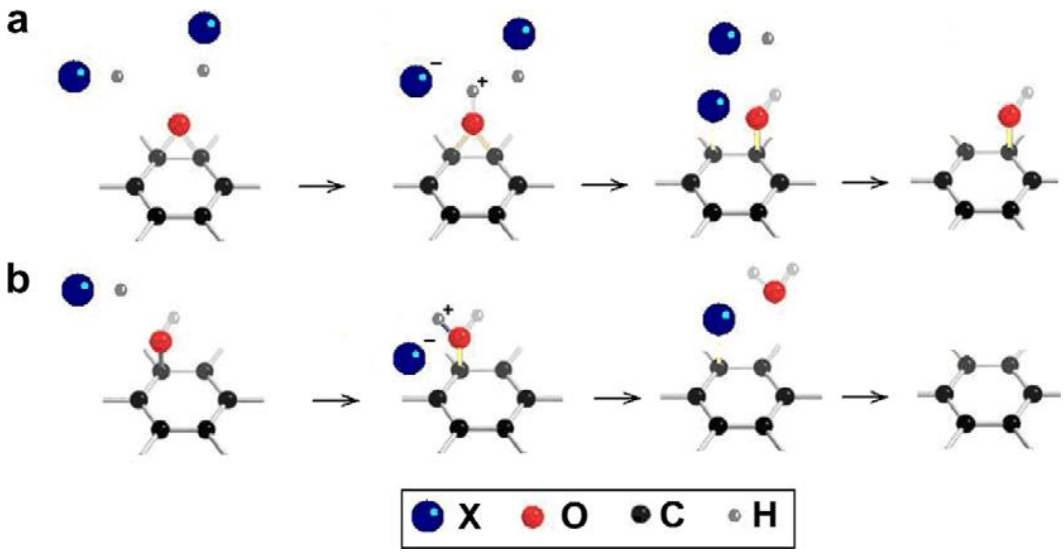

Figure A.1 Proposed reaction mechanism for Hydrohalic acid reduction of GO. (a) Ring-opening reaction of an epoxy group. (b) Halogenation substitution reaction of a hydroxyl group

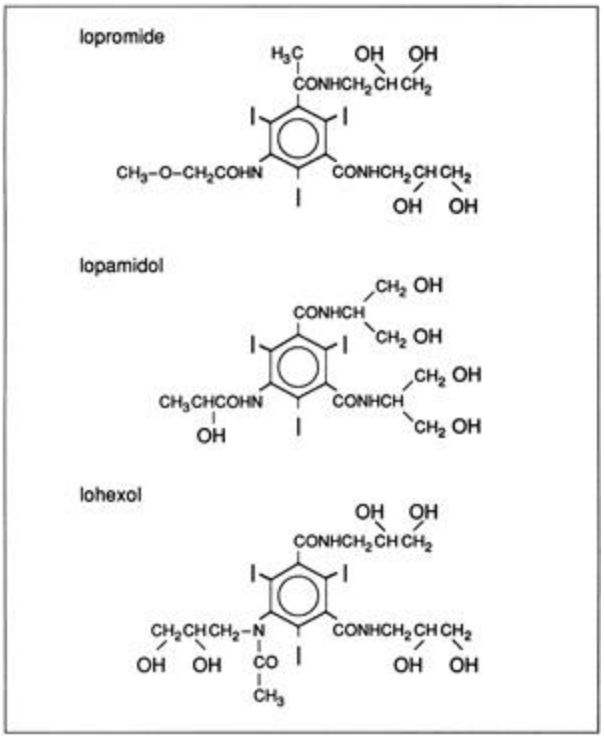

Figure A.2 Chemical structure of commercial CT contrast agents. Source: Torsten Almén and Peter Aspelin, Medcyclopedia™ Standard Edition, General Electric Healthcare

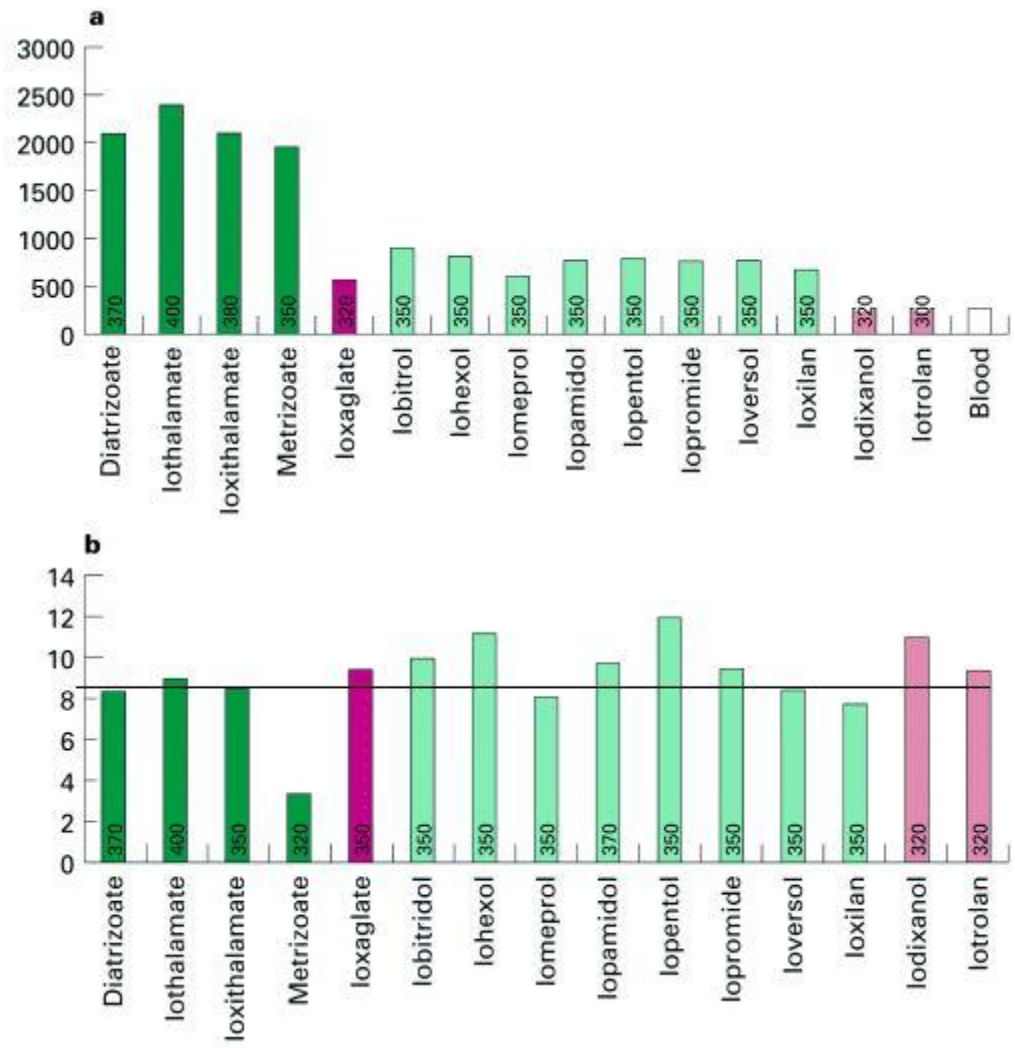

Figure A.3 Iodine content (mg/mL) for some commercial Iodinated CT contrast agents. Ionic High osmolality media - Green, Ionic Low osmolality medium- Red, Non-ionic Low osmolality media - light green and Non-ionic Iso-osmolality media - light red. Reprinted from literature [30].

Material	Elements			
	C1s	N1s	O1s	O/C ratio
GNP	99.35	—	0.65	0.006
GONP	66.3	0.45	33.25	0.501
Graphene	82.39	2.13	15.48	0.188

Table A.1 Atomic concentrations of Graphene Nanoplatelets, Graphite Oxide and Graphene. Reprinted from literature [26].